Australian Government
Department of Defence
Defence Science and
Technology Organisation

Reliability, Durability and Packaging of Fibre Bragg Gratings for Large-Scale Structural Health Monitoring of Defence Platforms

Claire Davis, Ivan Grabovac, James Kopczyk, Peter Lombardo, Patrick Norman, Anthony Rizk, Travis Nuyens and Silvia Tejedor

Aerospace Division
Defence Science and Technology Organisation

DSTO-TR-2880

ABSTRACT

This report documents an experimental program of work which investigates the reliability and durability of fibre Bragg gratings (FBGs) under tensile loading conditions and the factors which contribute to their ultimate performance. In addition, methodologies for broad-area permanent attachment of FBG sensing arrays are also investigated and two techniques are presented for proposed application in the structural health monitoring of Defence platforms.

Published by

Aerospace Division
DSTO Defence Science and Technology Organisation
506 Lorimer St
Fishermans Bend, Victoria 3207 Australia

Telephone: 1300 DEFENCE
Fax: (03) 9626 7999

AR-015-684
August 2013

APPROVED FOR PUBLIC RELEASE

Reliability, Durability and Packaging of Fibre Bragg Gratings for Large-Scale Structural Health Monitoring of Defence Platforms

Executive Summary

This report documents an experimental program of work which investigates the reliability and durability of fibre Bragg gratings (FBGs) under tensile loading conditions and the factors which contribute to their ultimate performance. In addition, methodologies for broad-area permanent attachment of FBG sensing arrays to Defence platforms are investigated and two techniques are presented for proposed application in structural health monitoring systems.

The work described in this report forms part of a contribution by the Defence Science and Technology Organisation (DSTO) to a three year research program on "Structural Health Monitoring Through Environmental Excitation and Optical Fibre Sensors" sponsored by the US Office of Naval Research (ONR) under a Naval International Cooperative Opportunities in S&T Program (NICOP). The program is supported by a collaborative research effort involving researchers from the US Naval Academy (NA), Naval Surface Warfare Centre (NSWC), the Australian Co-operative Research Centre for Advanced Composite Structures (CRCACS) and DSTO.

The ultimate goal of the overriding program is the demonstration and validation of a large area vibration-based structural health monitoring system on a composite sub-structure using simulated environmental excitation and a network of surface-mounted fibre Bragg gratings for response measurement. This is the subject of a separate report.

This page is intentionally blank

Contents

This page is intentionally blank

Glossary

ASE – Amplified Spontaneous Emission

AVIM - Aviation Intermediate Maintenance

CRCACS – Australian Co-operative Research Centre for Advanced Composite Structures

DSTO – Defence Science and Technology Organisation

DMI – Diamond Micro Interface

DTG – Draw Tower Grating

FBG – Fibre Bragg Grating

FOS&S - Fibre Optic Sensors and Sensing Systems

GFRP – Glass Fibre Reinforced Plastic

PI – Polyimide

NA – US Naval Academy

NSWC – Naval Surface Warfare Centre

RDM – Resin Distribution Medium

SIDER - Structural Irregularity and Damage Evaluation Routine

TDS – Technical Data Sheet

VARTM – Vacuum-Assisted Resin Transfer Moulding

This page is intentionally blank

1. Introduction

The use of Bragg gratings in optical fibres to measure strain was first reported in the literature in the mid 1980s [1]. Fibre Bragg Gratings (FBGs) offer a number of key advantages over existing strain sensing technology. They are immune to electromagnetic interference, are self-referencing and can support many different spatially separated sensors along a single optical fibre. The optical fibres can be embedded or surface–mounted on the host structure with minimal intrusion providing the potential for in-situ high-density distributed strain and temperature sensing. The intrinsic material properties of the optical fibre (Silica glass) also demonstrate excellent resistance to fatigue and corrosion.

Despite these advantages, there has been a relatively slow adoption of the technology within the aerospace field. This can be attributed to many factors; the equipment required to interrogate the sensors is costly and often sensitive to harsh environments, there is a lack of conclusive information about sensor reliability and durability and the existing electrical foil strain gauge technology is well-understood and suitable for most discrete sensing applications. Furthermore, there has been limited experience in the field with embedment, bonding and networking techniques for optical fibres particularly on large and/or complex structures.

This report details an experimental program of work which seeks to address some of the remaining engineering challenges associated with reliably surface-mounting broad-area FBG sensing networks to large structures. The three main steps in the creation of an FBG strain sensing network: fabrication, packaging and bonding and their respective contributions to the ultimate strength and durability of the system are investigated.

2. Broad-area Packaging Techniques

Much of the documented research covering structural health monitoring (SHM) applications using distributed optical fibre based sensing systems has focused on large structures where the application of a distributed, non-intrusive sensing system is most advantageous. The detail pertaining to this research has usually focused on the interrogation and analysis methodology for the FBG's rather than the processes for actually applying these sensor arrays to the structure and making reliable measurements. In fact, there is very little research in the published literature relating to practical techniques for incorporating distributed FBG arrays into or onto structures and the majority of commercially-available packages for FBG sensors have been developed for single point measurements of strain and/or temperature. For broad-area structural assessment and health monitoring of large Defence platforms, a robust and reliable technique is required for surface-mounting a network of sensors onto a large structure, as represented schematically in Figure 2.1.

Some of the field issues for large-scale applications are:

- **Pre-packaging**: For large-scale sensor applications where hundreds of sensors can be used, a new way of sensor handling and placement must be developed. A single fibre up to 5 or 10 m in length may have many sensors in the array; therefore from a practical viewpoint the pre-packaging should involve some form of fibre shielding to protect fibres during handling and transportation as well as a methodology for accurately positioning each sensor.
- **Transportation** schemes for large numbers of FBG sensors to the site of application should be designed to avoid mechanical damage and allow for ease of onsite application.

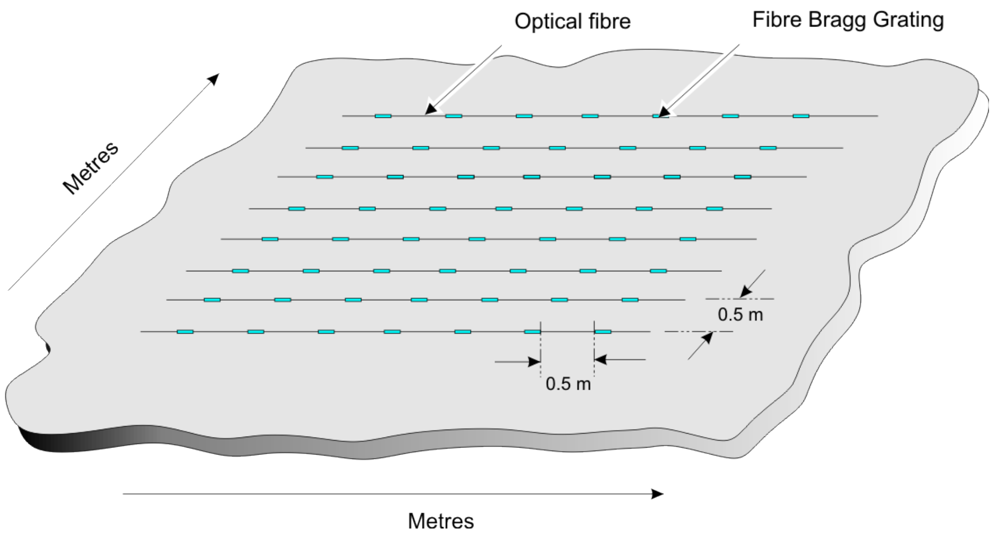

Figure 2.1: Schematic representation of a typical sensor distribution over a representative structure surface.

- **Alignment** of the optical fibre arrays should in principle form a pattern of coordinates consistent with those of a structure for easier damage location and identification.
- **Packaging and Mounting** must ensure realistic strain transfer to the sensor(s), i.e. the use of the bonding medium must not contribute to relaxation or creep under load. Generally, thermo-set resin systems are considered suitable for this application as there is no measurable material distortion after full cure.
- **Protection** of the sensor system installed on a structure against damage due to abrasion, mechanical interference, environmental effects or any combination thereof must be considered. Unless temperature measurements are required, the protection should ideally insulate against environmental temperature extremes to minimize temperature effects on the strain measurement or alternatively some means of temperature compensation should be considered. Protection of the sensor system from environmental effects, such as moisture ingress and UV degradation, is very important especially should such a system be used over extended periods (years).

With these considerations in mind, two different packaging techniques were developed at DSTO to facilitate the broad area application of FBG arrays to Defence platforms. The first technique was a vacuum assisted resin transfer moulding (VARTM) process; the second technique involved curing the optical fibre into a resin impregnated nylon carrier tape (Redux® 312). This tape can either be co-cured with the structure or cured separately with the optical fibre and then secondarily bonded to the structure.

Both packaging techniques are suitable for broad area surface mounting of FBG arrays. The VARTM technique is applied at room temperature and has a thickness of 1–3 mm depending on the resin distribution medium. The Redux tape has a lower impact on the surface profile of the structure (400–600 μm) but can only be applied to materials which can withstand temperatures of 120 °C if co-cured directly to the structure. Some further details about both packaging techniques are given in the proceeding sections of this report.

2.1 VARTM Packaging

VARTM is a closed moulding technique where a vacuum pressure draws the resin along a distribution medium [2]. It is typically a three-step process including the lay-up of reinforcing fibre pre-form, pre-form impregnation with resin, and ambient or elevated temperature resin cure. A fibreglass test coupon, showing on a small-scale, the various layers used in the VARTM process developed for the surface attachment of optical fibres is shown in Figure 2.2.

The first layer of the VARTM system is a pressure sensitive, self-adhesive tape used for placement, transportation and temporary adhesion of the optical fibre network. The second layer is a peel ply which is generally used in VARTM for separation of the resin distribution media from the structure after resin cure. The third layer of the VARTM lay-up acts as the resin distribution medium. The resin system used was a low-viscosity thermoset system designed to achieve good wetting, high-strength and low-creep adhesion. Many commercially-available adhesives were sourced and trialled during the packaging development process [3]. The final selection was an epoxy laminating resin system, available locally from Fibreglass International (FGI), Resin: R180, Hardener: H180 slow®.

Depending on the vacuum pressure applied, the infusion time using these pre-form materials is approximately 5-10 minutes for a 1.5 cm x 6 cm infusion area. For large-scale infusions the VARTM lay-up process was modified by incorporating multiple resin injection ports and replacing the resin distribution medium shown in Figure 2.2 with one which had a more open structure to speed-up the resin infusion process. Figure 2.3 shows the laboratory trials for a 3 meter infusion with three embedded optical fibres.

® A product of Fiber Glass International (FGI) Australia, http://www.fgi.com.au/files/images/stories/pdfs/products/resins/Epoxies.pdf

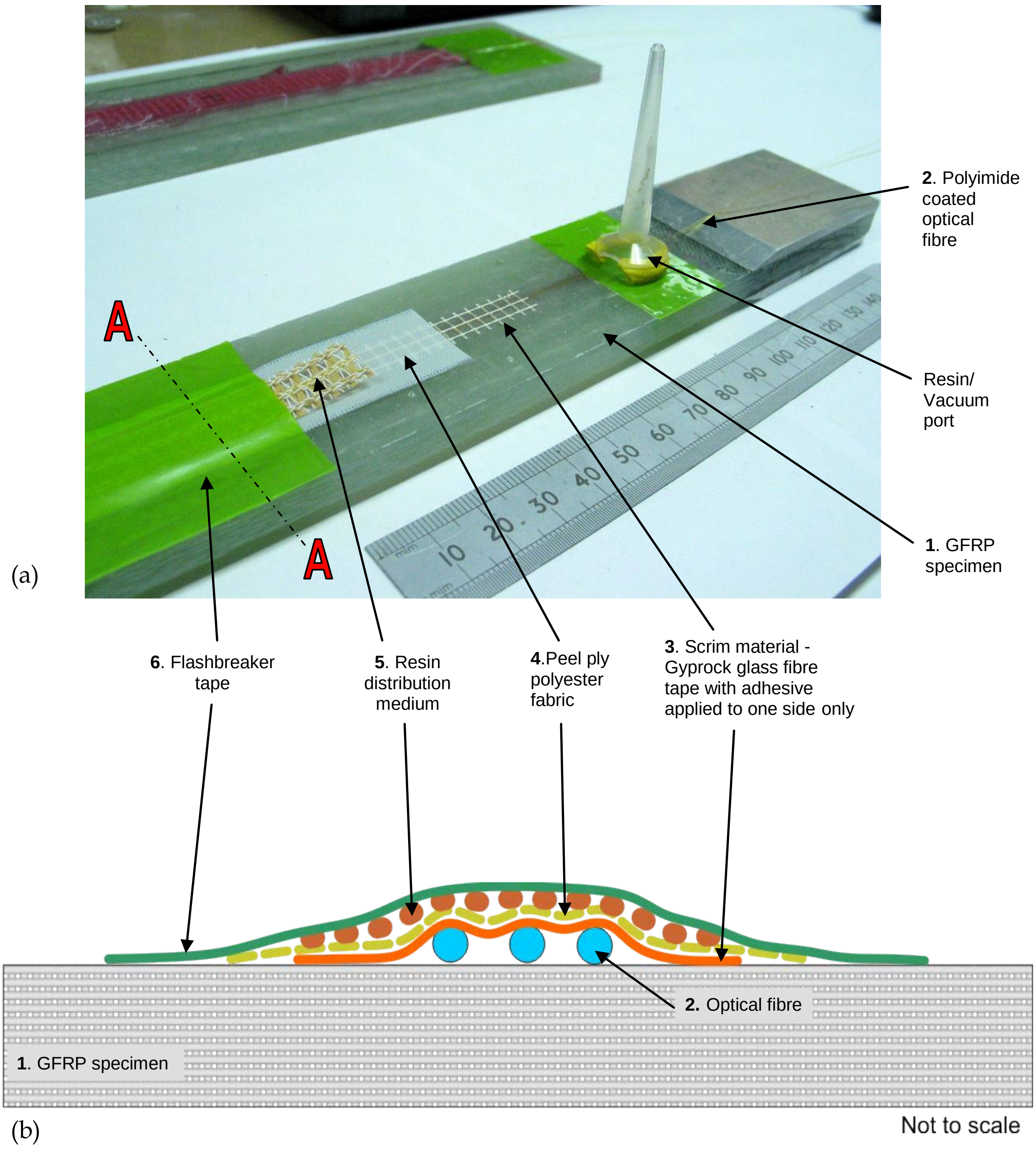

Figure 2.2: Typical lay-up for resin infusion and bonding of FBG sensors to glass fibre reinforced plastic (GFRP) test specimen (lay-up order from bottom to top). (a) All materials used in mini-VARTM; (b) Cross-sectional view at point A-A. Note, after resin infusion and cure the layers 4, 5 & 6 are removed.

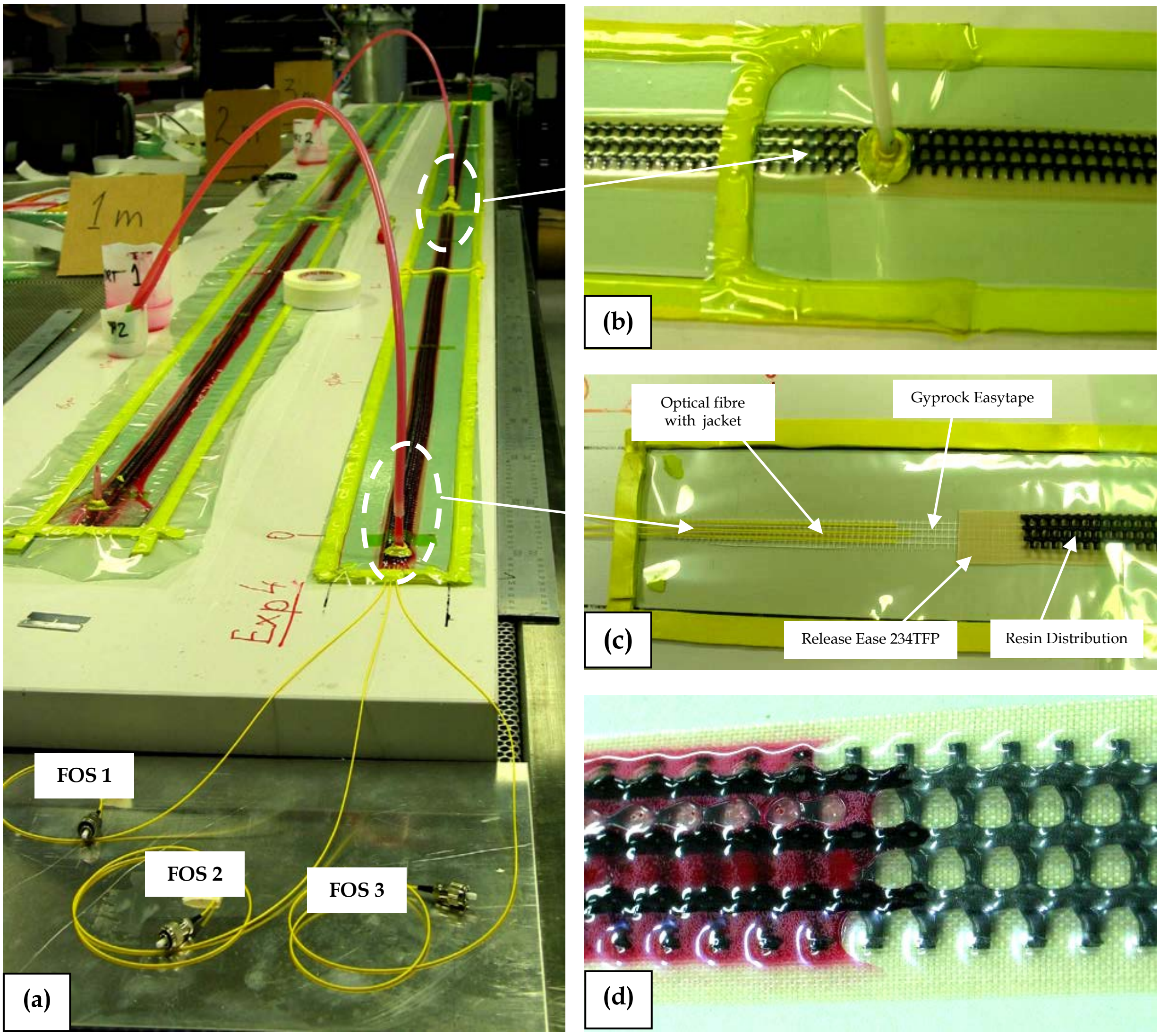

Figure 2.3: (a) Large-scale VARTM simulation; (b) 2nd injection point detail; (c) Lay-up detail; (d) Close-up of advancing resin front.

2.2 Redux Tape

The second packaging technique developed utilizes a nylon woven carrier tape impregnated with a modified epoxy film adhesive (Redux® 312). This material was originally designed for maintaining uniform bond line thickness in composite to composite bonding applications for the aerospace field. The optical fibres are firstly laid up under tension beneath several plies of the film adhesive tape in a mould as shown schematically in Figure 2.4. The number of plies of film adhesive can be varied to suit the thickness and flexibility required for the tape. A single ply will result in a tape thickness of approximately 250 μm while two plies will result in a thickness of approximately 440 μm. The Redux film layer(s) are then covered with a vacuum film and sealed as shown in Figure 2.4(b).

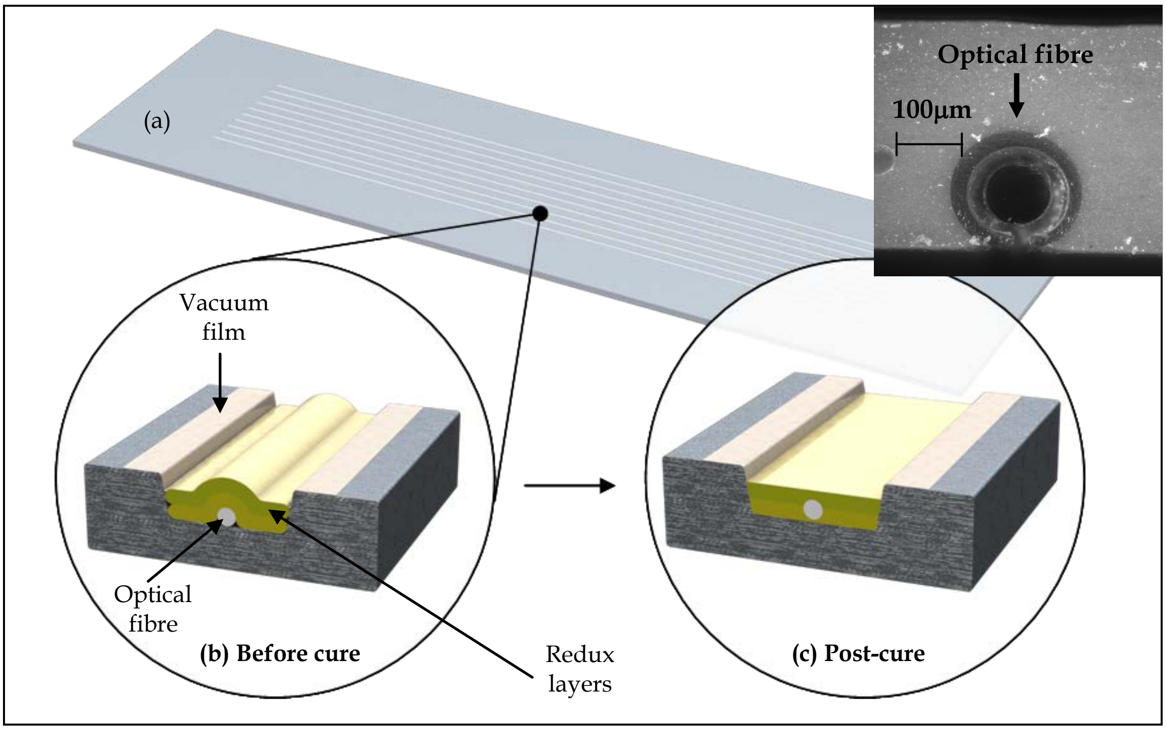

Figure 2.4: (a) Aluminium mould for fabrication of Redux tape with embedded optical fibres; (b) Schematic representation (side profile) of two-ply lay-up for embedment of optical fibre in Redux tape before cure; (c) After cure. Inset (cross section of Redux tape after cure).

The film is cured at 120 °C under vacuum resulting in a thin flexible tape with a very thin resin layer between the fibre and the bottom-side of the tape as shown in the inset of Figure 2.4. This tape can then be secondarily bonded to the structure using standard aerospace grade strain gauge adhesive (M-Bond 200 or AE-10) or cured directly to the parent structure as shown in Figure 2.5.

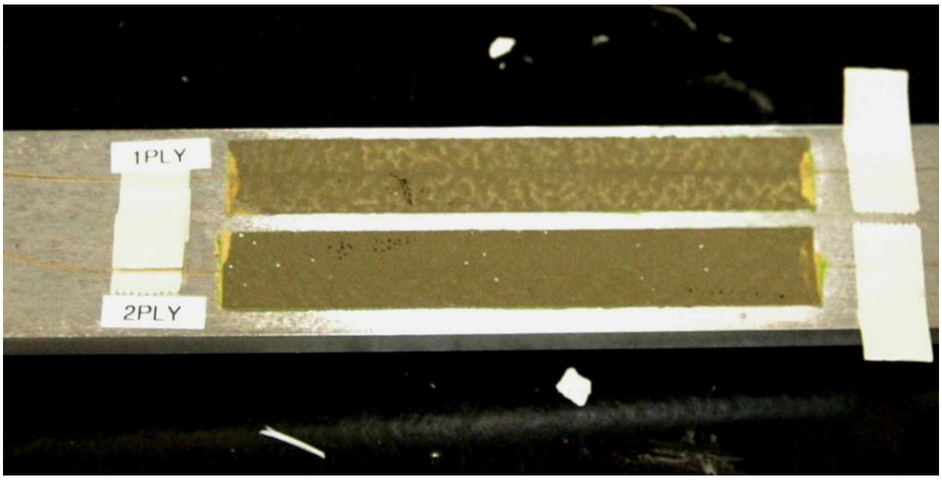

Figure 2.5: Single and two ply Redux tape with embedded optical fibres shown cured directly to Aluminium sample.

If the embedded optical fibre has an outer (900 μm) jacket, the transition between jacketed and bare fibre is accommodated at the edges of the tape by building up with additional plies of film adhesive tape and strain relief at the egress points is provided using pressure sensitive sealant tape (SM5153 Tacky Tape®) as shown in Figure 2.6. The operating temperature of the Redux® tape is up to 212 °F (100 °C). A higher temperature variant of this tape is also available (Redux® 322), which is cured at 350 °F (175 °C) using the same methodology and is suitable for operating temperatures up to 390 °F (200 °C) [4].

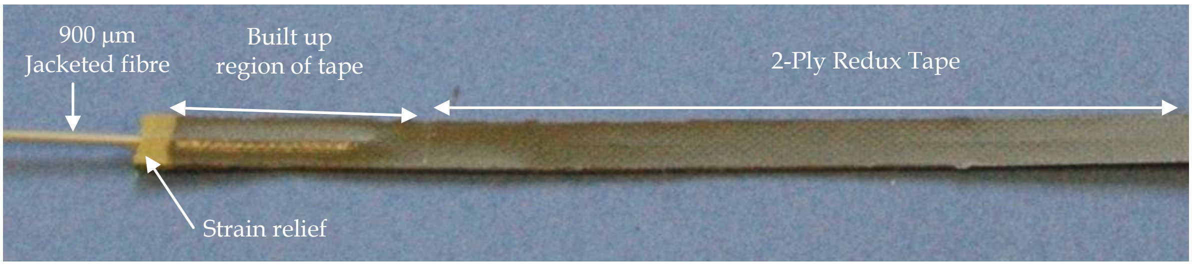

Figure 2.6: Close-up of the cured Redux tape showing built-up egress point of jacketed optical fibre from Redux tape.

The tape may be cured in an oven using a core plate such as that shown in Figure 2.7 or alternatively using a thermal blanket as shown in Figure 2.8 which facilitates the fabrication of long tape lengths without the requirement for a large oven. A thermal blanket may also be used for in-situ thermal cure directly to the structure as long as the parent structure can tolerate the curing temperature.

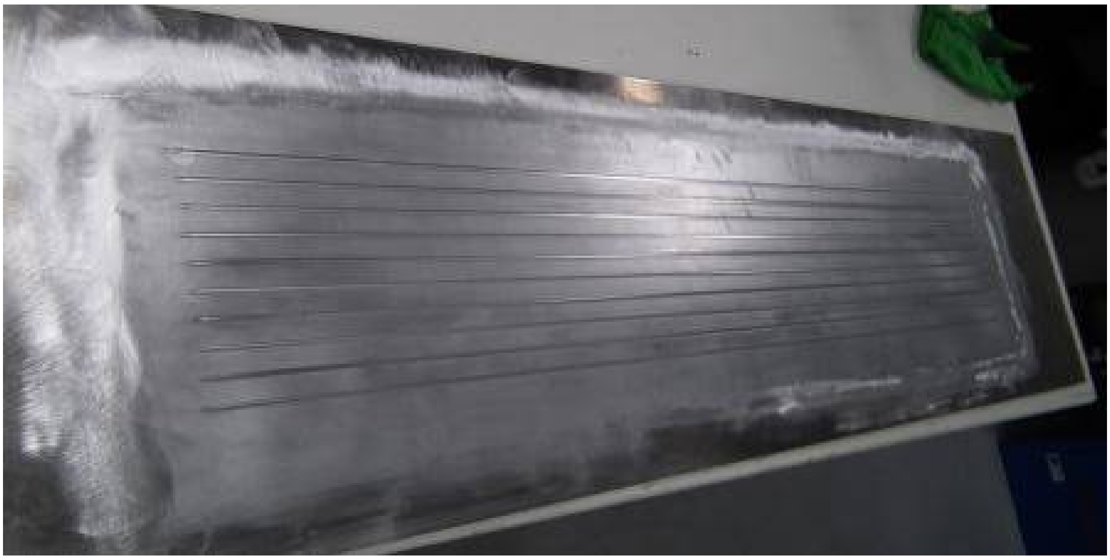

Figure 2.7: Aluminium mould used to lay up and cure Redux tape with embedded optical fibres.

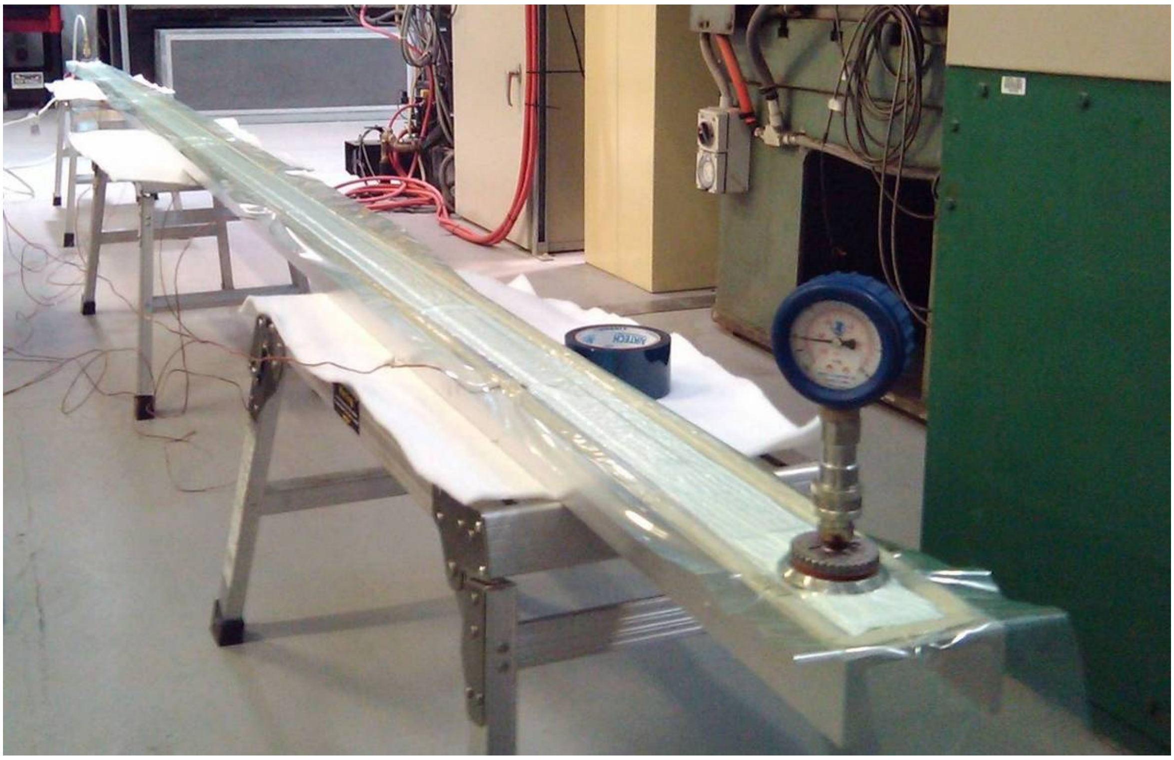

Figure 2.8: Photograph showing 5.5 metre length of Redux tape under vacuum bag, being cured using a thermal blanket.

3. Optical Interconnects

An important part of the process of installing an optical fibre sensing network is the consideration of optical interconnects. Typically the optical fibre exits the structure and is connected to the interrogation equipment via an optical fibre patch cord. The egress point of the compliant optical fibres from the stiff structure is a well established mechanical weak point. A more robust approach is to incorporate the optical fibre connectors and mating adaptors into the part to facilitate optical interconnects to the interrogation apparatus or to a fibre optic communications bus post-installation on the structure.

For most large platforms after the primary sub-structures have been fabricated, they are typically over-coated. This coating has no structural element and is used only to provide environmental protection to the underlying material and sometimes enhance shape and reduce observability. By surface mounting the FBG arrays to the structure after fabrication of the part but prior to application of the protective layer, any potential issues with re-certification of the part due to the inclusion of the optical fibres can be avoided and additionally the fibres are protected by the outer layer. Figure 3.1 shows a schematic diagram of the proposed installation process.

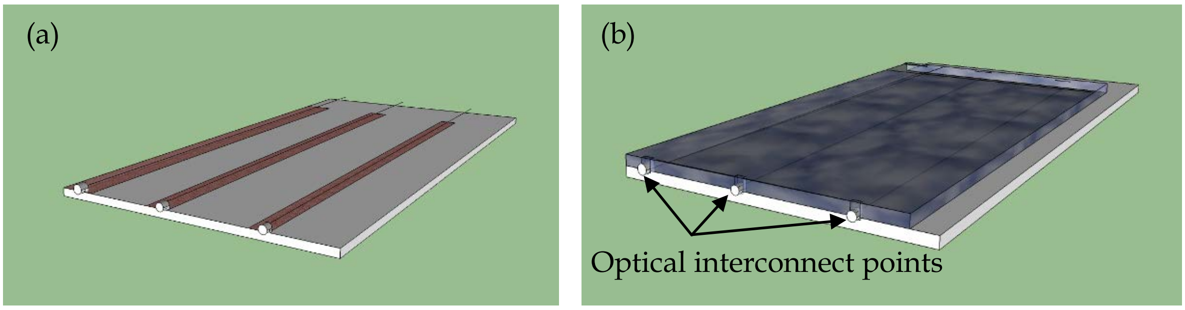

Figure 3.1: Schematic diagram representing lay-up process including connectors for optical fibre sensing network. (a) Surface mounting of optical fibre array, connectors, mating adaptors and packaging; (b) Over-coating of protective layer.

The thickness of the protective layer can vary from less than a millimetre to several centimetres depending on the structure and its environment. For greatest flexibility and to minimise intrusion, a connector and mating adaptor with as small a cross-section as possible should be utilised. In the initial stages of development a low-profile DMI (Diamond Micro Interface) optical fibre connector with a cross-section of 2.7 mm was tested as shown in Figure 3.2(a). These connectors were originally developed for optical interconnects on printed circuit boards. Figure 3.2(b) shows a DMI connector and mating adaptor embedded in a Versalink™ coating on an E-glass vinyl ester composite coupon to demonstrate the principal of the embedded connector.

Because the in-service application for this work is initially planned to be in the maritime domain the insertion loss for the connector and mating adaptor was tested for connections made while submerged in water. This testing was performed in both fresh and sea water for a series of 20 disconnects and reconnects. The results are plotted in Figure 3.3 demonstrating the ability to make an optical connection in an underwater environment.

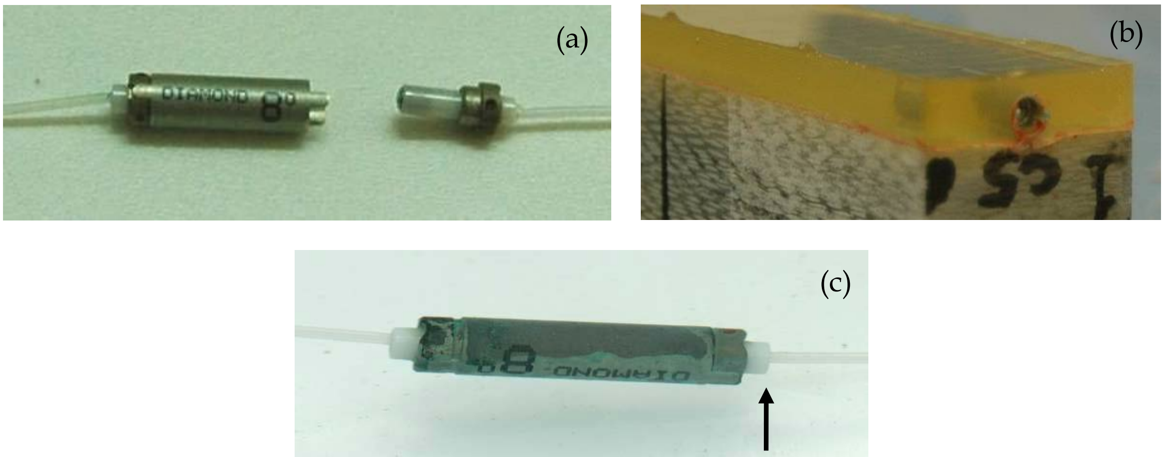

Figure 3.2: (a) Photograph of DMI connector and mating adaptor; (b) Cross-section of composite lay-up showing E-glass/vinyl ester plies and protective resin coating with embedded connector; (c) Corroded connector and mating adaptor (after 12 months immersion in seawater) with arrow indicating mechanical weak spot.

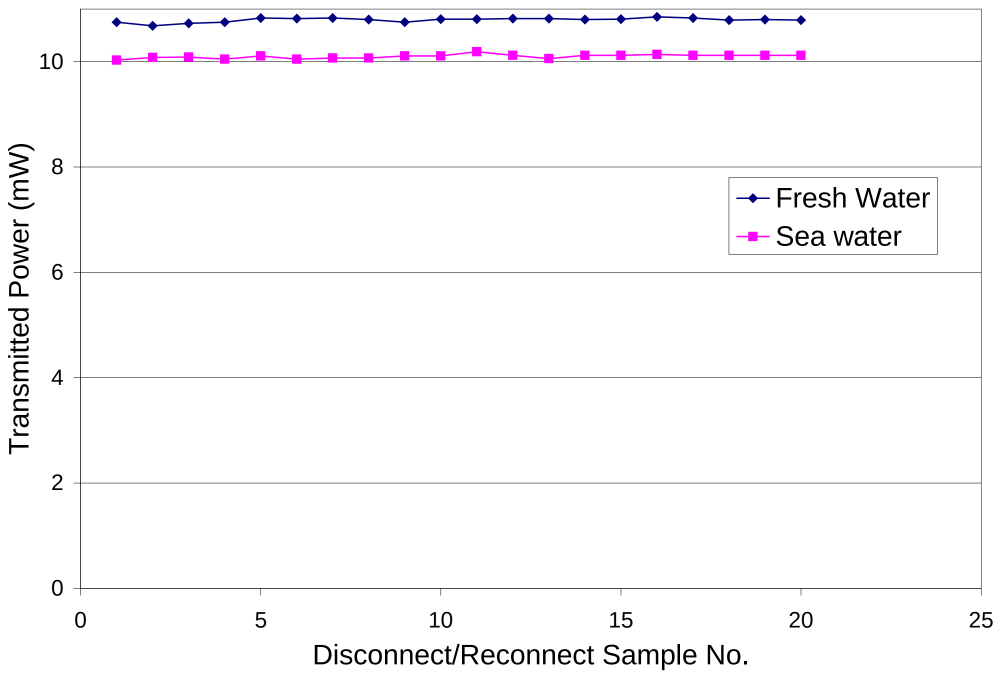

Figure 3.3: Transmitted intensity through two DMI connectors and a mating adaptor (as shown in Figure 3.2 (a)) for a series of submerged disconnect/reconnect tests in fresh and sea water.

The long-term performance of this type of connector in seawater was also investigated over a period of 18 months. This underwater testing revealed that the Nickel plated mating adaptors were corrosion prone and in addition, there was a mechanical weakness at the join from the jacketed fibre to the connector as indicated in Figure 3.2(c). In order to alleviate the corrosion issues and address the mechanical weak spot on the connector, a custom designed low-profile connector was designed in titanium in collaboration with the manufacturer of the original low-profile connector (Diamond SA).

The new mating adaptor was a hybrid design incorporating elements from the original low-profile DMI and a mini AVIM (Aviation Intermediate Maintenance) assembly which was designed for NASA to facilitate high performance optical interconnects in harsh space environments. The low-profile DMI side of the adaptor is designed to be embedded within the protective layer of the part while the spring-mounted AVIM assembly is external to the part to facilitate the optical interconnect. The connectors are keyed to ensure consistent mating and the spring mounted assembly incorporated on the exposed side of the mating adaptor maintains precise ferrule to ferrule contact in harsh thermal and vibration environments. The exposed connector side also incorporates a ratchet mechanism to ensure the interrogation fibre does not come loose over time. Figure 3.4 shows the schematic for this hybrid connector assembly. The preliminary results from underwater tests using these new connectors are outlined in the proceeding paragraphs. Long-term testing of the performance of these connectors and their suitability for embedment in the protective layer of a structure is continuing.

Preliminary testing using off the shelf titanium AVIM mating adaptors supplied by the manufacturer showed that, as expected, this material offers much enhanced resistance to corrosion during submersion in sea water. However these titanium mating adaptors had an austenitic stainless steel (X10CrNiS189) alignment pin in their assembly. Figure 3.5(a) shows that after 4 months of submersion, the steel pin in this mating adaptor showed evidence of significant corrosion. The customised titanium mating adaptors, which were supplied later, replaced the stainless steel alignment pin with one fabricated from Grade 5 Titanium. These were tested underwater for an extended period without any visible sign of corrosion as shown in Figure 3.5(b). In this case, the use of a purely titanium construction is necessary to avoid galvanic corrosion issues.

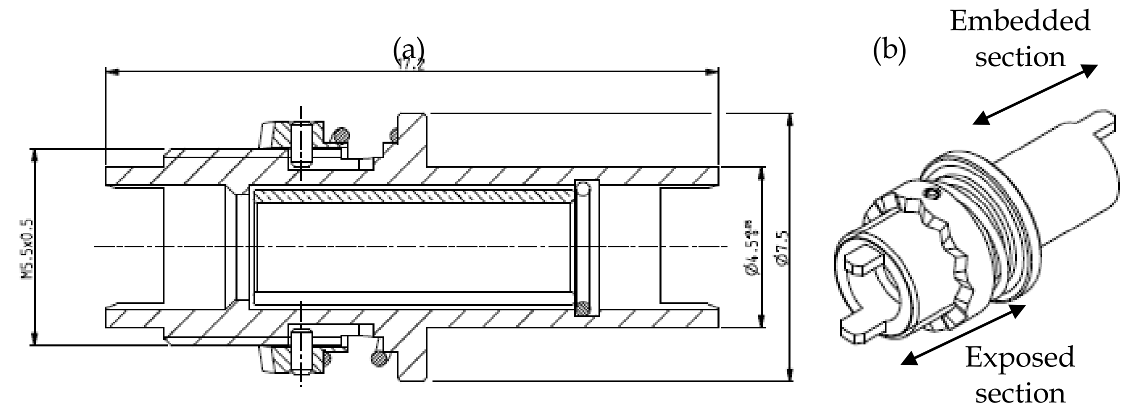

Figure 3.4: (a) Schematic showing the detail of the customised hybrid AVIM/DMI connector; (b) Sketch of the connector indicating section of the mating adaptor which is embedded and section which is exposed to facilitate interconnects.

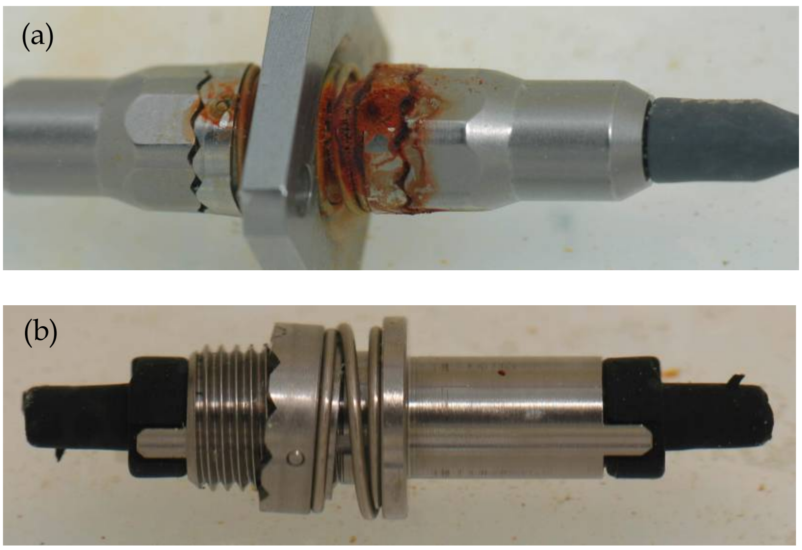

Figure 3.5: (a) Photograph of off-the-shelf steel pinned titanium connector undergoing corrosion after 4 months submersion in sea water; (b) Photograph of customised entirely titanium low profile connector after 6 months submersion in sea water — no corrosion present.

4. Fabrication Techniques for Fibre Bragg Gratings

As outlined in the introduction, an FBG is a periodic change in refractive index in the core of an optical fibre. The periodic modulation is achieved by exposing the fibre (side-on) to interference fringes from a UV laser beam. The region of the optical fibre exposed to the beam is altered via modification of the oxygen vacancy-defect absorption band resulting in a small increase in refractive index. Because the protective coating on the optical fibre is typically not transmissive to UV light it is usually removed prior to exposure by the UV laser beam.

There are typically four main steps involved in fabrication of a fibre Bragg grating:

1. Removal of the fibre coating.
2. Photosensitization of the fibre.
3. Exposure of the grating to UV laser light.
4. Annealing and Re-coating/packaging.

Steps 1 and 2 can be interchangeable depending on the coating removal process but each one of the steps in the process has the potential to introduce structural flaws to the glass surface which weakens the fibre's ultimate strength and long-term reliability. For high density strain sensing applications where the coating must be removed at many sections along the same fibre to inscribe multiple gratings, there is a much higher chance of the fibre being damaged at some point along its length. Nearly all of the commercially-supplied gratings are currently fabricated in this way.

FBGs may also be inscribed during the optical fibre fabrication process; these gratings are commonly referred to as draw-tower gratings (DTGs). Historically, DTGs were characterized by very low reflectivities (< 1%) due to the fact that there was a limited time window available for UV exposure during the fibre draw process. In recent years, with the advent of new strongly photosensitive glass materials and fibre draw-speeds which can be well-controlled over slower rates, DTGs have become commercially available with reflectivities up to 30 – 50% [5].

Figure 4.1 shows a schematic diagram of the production process for a DTG which involves a series of steps as outlined below:

1. The photo sensitive glass pre-form is heated up and drawn to initiate the formation of the fibre.
2. The drawn fibre crosses the optical axis of a pulsed Excimer laser which uses an interferometric technique to expose the fibre to a periodic UV exposure pattern.
3. The fibre draw speed is monitored in combination with the laser pulse to control the exact location of the FBG sensors.
4. The fibre is then coated in the draw tower using a standard fibre coating process.

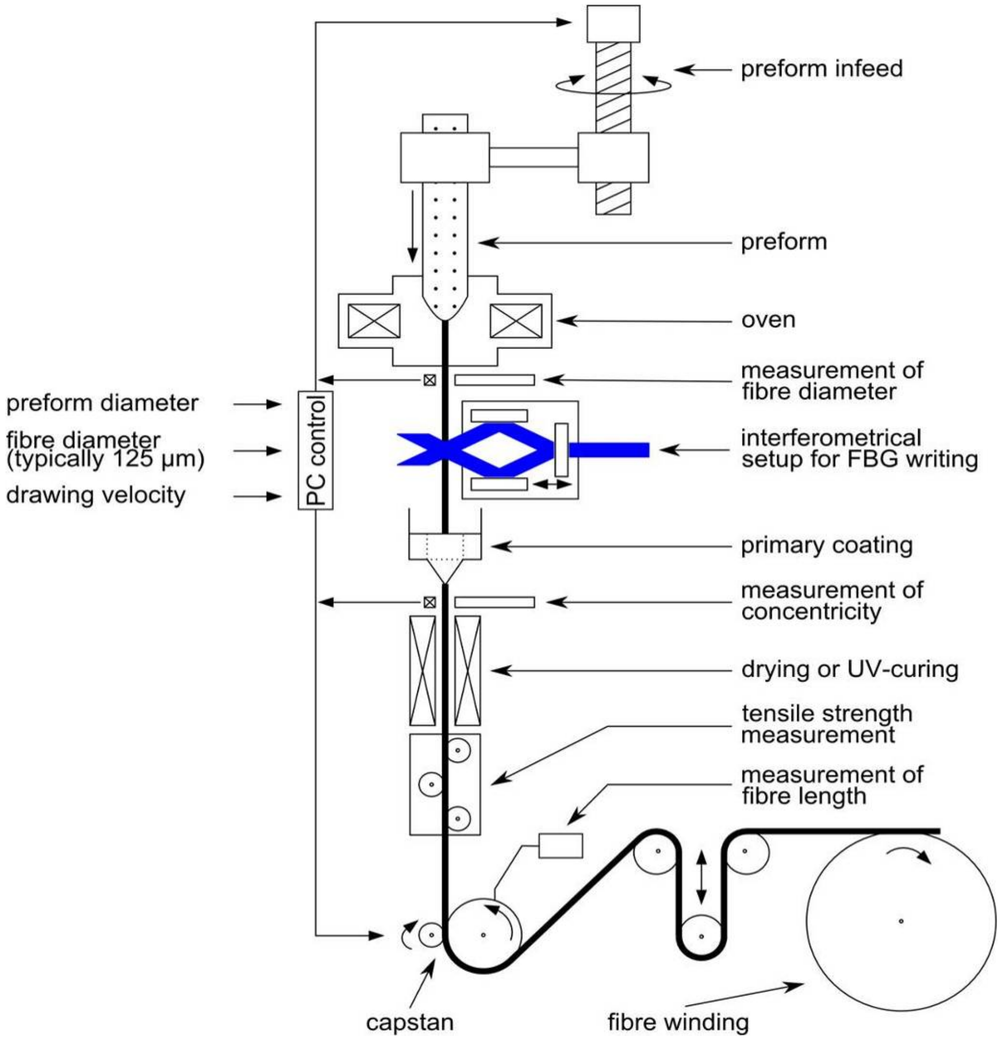

Figure 4.1: Schematic representation of draw tower set-up (Diagram supplied courtesy of FBGS International).

DTGs should in theory result in enhanced durability and increased strength because of the fact that the FBG is written immediately before the protective coating is applied to the fibre, which minimizes the potential for contamination of the exposed glass and avoids the requirement for harsh coating removal techniques.

4.1 Optical Fibre Coating Removal Techniques

Optical fibres are typically coated to provide a hermetic seal which provides environmental and mechanical protection. The two most common coatings are UV cured acrylate and polyimide (PI). Acrylate is relatively low-cost, easy to apply in the fibre draw tower, offers good environmental stability and can also be easily removed mechanically. However the adhesion of the coating to the glass is not strong and the operating temperature range is limited to between -65 and 85 °C. Conversely, PI coatings will not dissolve in most organic solvents or be removed using conventional fibre coating removal tools or techniques. It is chemically bonded to the glass surface and has excellent adhesion and good mechanical properties. It also provides an extended operating temperature range (-60 to 300 °C). For these reasons PI coated fibres are generally used for sensing applications in harsh environments which may experience extreme temperatures. However these qualities also mean that the techniques required to remove the PI coatings are often harsh and can introduce defects or damage prior to inscription of the grating. The FBG inscription process requires the removal of this coating which has been reported to reduce the mechanical strength of the optical fibre [6]. For the purposes of this investigation five different coating removal methods for optical fibres were investigated.

4.1.1 Thermal wire stripper

A thin shaped heating element (900 °C) melts the PI coating which is then pulled away from the top of the fibre. This tool, shown in Figure 4.2, was originally designed for electrical cabling to remove the insulation layer without nicking the conducting wire beneath, but may also be used for stripping the PI coating from optical fibres.

Figure 4.2: Photograph of a thermal wire stripper.

4.1.2 Butane Flame

A low temperature/high oxygen mix butane flame (cigarette lighter) burns the PI coating, leaving a carbon residue which requires cleaning using alcohol and lint-free wipes. This is one of the easiest and most common methods of removing the PI coating from an optical fibre.

4.1.3 Butane torch

A high temperature (up to 1400 °C) butane flame from a pressurised canister thermally ablates the PI coating. The device is shown in Figure 4.3. The temperature of the flame is adjusted by controlling the butane/oxygen mix to ensure a temperature which is high enough to vaporise the PI coating without melting or softening the glass beneath.

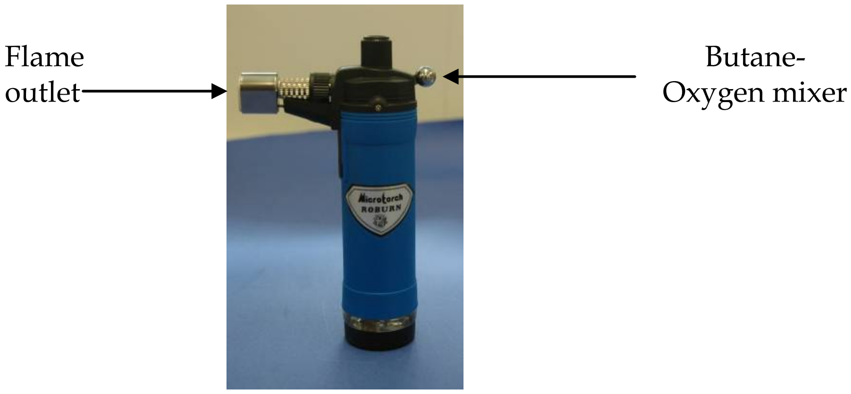

Figure 4.3: Photograph of Butane torch with temperature control

4.1.4 CO_2 laser ablation

Laser ablation of the coating was conducted using a commercially supplied CO2FMS CO_2 Laser stripping system (Oz Optics) as shown in Figure 4.4. A 100 W CO_2 laser beam at 9.3 µm is focused on the fibre to ablate the coating. The fibre must be rotated in the field of the beam to ensure uniform coating removal.

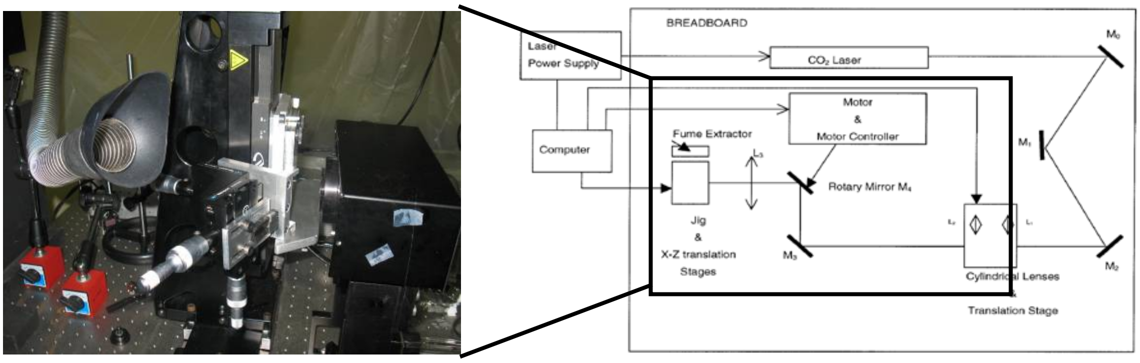

Figure 4.4: (a) Photograph showing detail of fibre stripping area; (b) Schematic diagram of laser stripping apparatus.

4.1.5 Heated Sulphuric Acid

The fibre is immersed in concentrated (99.9%) sulphuric acid at 120 °C for 20 minutes to chemically remove the PI coating. Faster removal times are possible at higher temperature but acid fuming and irregular removal rates can occur. The setup of the heated sulphuric acid stripping method developed for this testing is shown in Figure 4.5. A stepper motor controller has been used so that the entire process can be conducted in a fume cupboard.

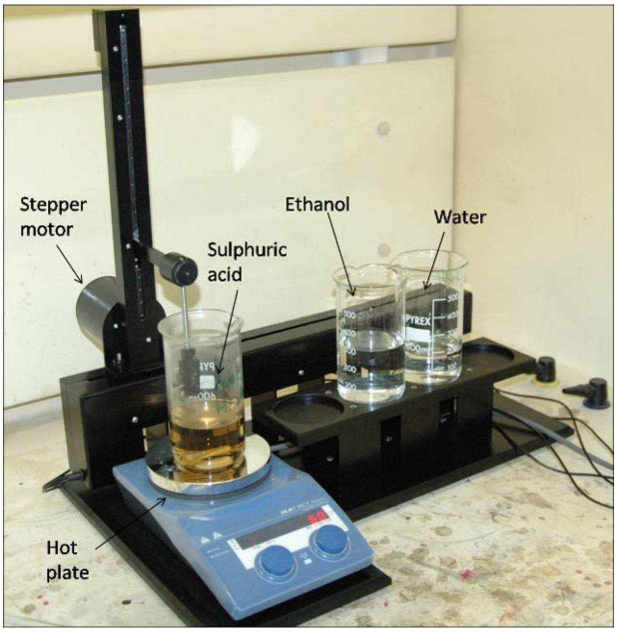

Figure 4.5: Experimental apparatus for heated sulphuric acid stripping method. After immersion in the acid bath, residual acid is removed by immersion in an Ethanol and then a water bath.

4.2 Photosensitisation of the Optical Fibre

The intrinsic photosensitivity of the optical fibre is governed by the dopant materials in the glass however the photosensitivity can be enhanced by a process of high-pressure molecular hydrogen loading (H_2 loading) in a heated pressure vessel. Photosensitisation results in a stronger refractive index contrast for a given exposure time/laser power. This in turn can reduce the effects of environmental changes or beam instabilities during the writing process, because the required exposure time is reduced.

If possible, the removal of the fibre coating is carried out after the photosensitisation stage so that the fibre surface can be protected while in the heated pressure vessel. However if heat is required to remove the coating, this will cause out-gassing of the hydrogen in the fibre which will result in reduced and irregular photosensitivity of the fibre. For this reason most Bragg gratings written in PI coated fibres have their coatings removed prior to photosensitisation.

A custom-designed mounting assembly was developed to store the stripped fibres during hydrogenation and prior to inscription to ensure that any accidental physical contact of the exposed glass surface is avoided. The mounting assembly suspends the stripped section of the fibre in air between foam block mounts as shown in Figure 4.6 (a). The stripped fibres were hydrogenated for five days to photosensitise the fibre prior to grating inscription using a standard phasemask exposure technique [7]. All the fibres were stored in a desiccator cabinet, as shown in Figure 4.6 (b), post inscription and prior to packaging to minimise moisture ingress to the exposed glass. The fibres were packaged within 48 hours of inscription.

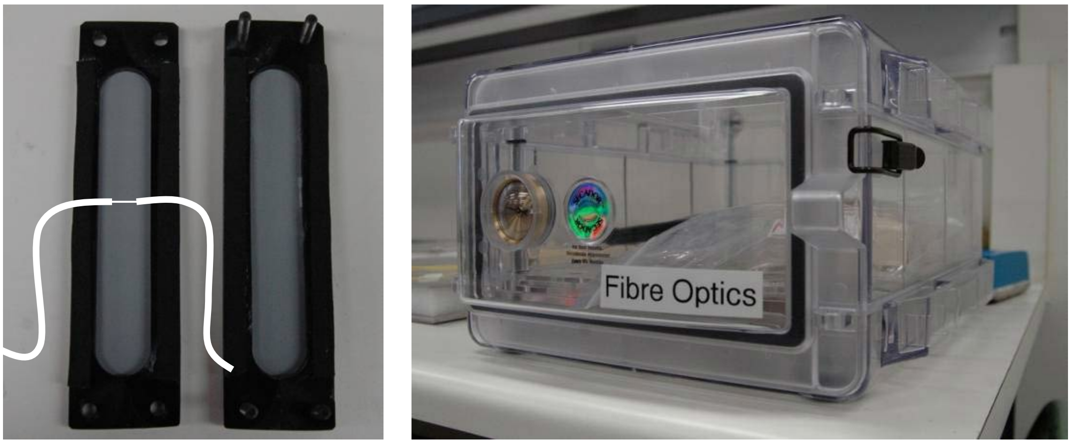

Figure 4.6: (a) Container (shown open) for suspending stripped optical fibres prior to packaging with a schematic representation showing location of a stripped optical fibre; (b) Desiccant container for storing stripped optical fibres.

5. Reliability and Durability Testing

The reliability and durability testing was conducted in two stages. Firstly, the performance of FBGs manufactured in fibres which had their coating removed using a variety of different coating removal techniques was investigated. The second stage of testing compared the performance of the best performing stripped FBGs to commercially supplied DTGs using both of the broad area packaging techniques which are described in Section 2, modified for smaller scale coupon tests.

5.1 Coupon Design

Two types of glass fibre reinforced plastic (GFRP) coupons were fabricated for the testing program using MTM57 E-glass pre-preg. The first coupon design comprised 12 unidirectional plies $[0]_{12}$ with dimensions of 200 mm × 25 mm manufactured to American Society for Testing and Materials (ASTM) Standards (D3039). The second coupon design comprised 12 plies laid up in a cross-ply orientation $[(+45,-45)_3]_s$ with dimensions of 200 mm × 25 mm also manufactured to ASTM standards. Aluminium grip tabs were bonded to each coupon, as shown in Figure 5.1, to protect the coupon from the load-cell grips during tensile loading in a mechanical test machine. The uni-directional test coupons had a predicted strain-to-failure of 20,000 $\mu\varepsilon$ with a linear stress-strain response curve to the yield strain at approximately 18,000 $\mu\varepsilon$. The cross-ply coupons had a much higher strain-to-failure (8% or 80,000 με), with a non-linear response beyond the yield point of the material at approximately 1,000 με.

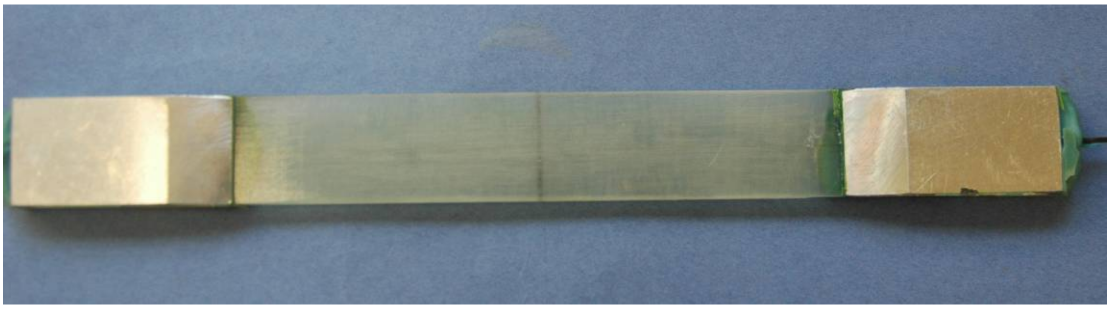

Figure 5.1: GFRP test coupon.

5.2 Modifications to Fibre Packaging for Coupon Tests

5.2.1 Vacuum-Assisted Resin Transfer Molding (VARTM)

The VARTM packaging technique outlined in Section 2 was adapted to allow for resin infusion on a smaller scale as detailed in the following steps. Firstly, the optical fibre containing the FBG is placed under tension on the test coupon. The first layer comprising self-adhesive tape (Gyprock Easytape™) is then applied to prevent fibre movement during the infusion process as shown in Figure 5.2.

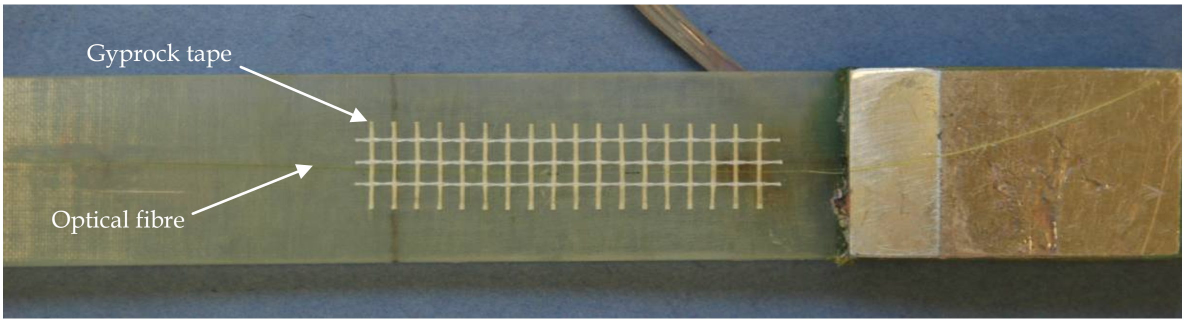

Figure 5.2: Stage one of the VATRM bonding technique (positioning the fibre).

The second layer, the peel ply, is a highly permeable fabric coated with Teflon which allows the upper layers of the preform and excess resin to be removed from the coupon after curing. The third layer is a coarse weave fabric which acts as the Resin Distribution Medium (RDM). This fabric is only used as the RDM for small scale infusions, for larger infusions an open wave black plastic mesh is used as the RDM. The peel ply and the RDM are placed on top of the Gyprock glass fibre tape. Then a seal is created around the Gyprock tape using a pressure sensitive vacuum sealant tape (Schnee Morehead SM5153 Tacky Tape®) as shown in Figure 5.3.

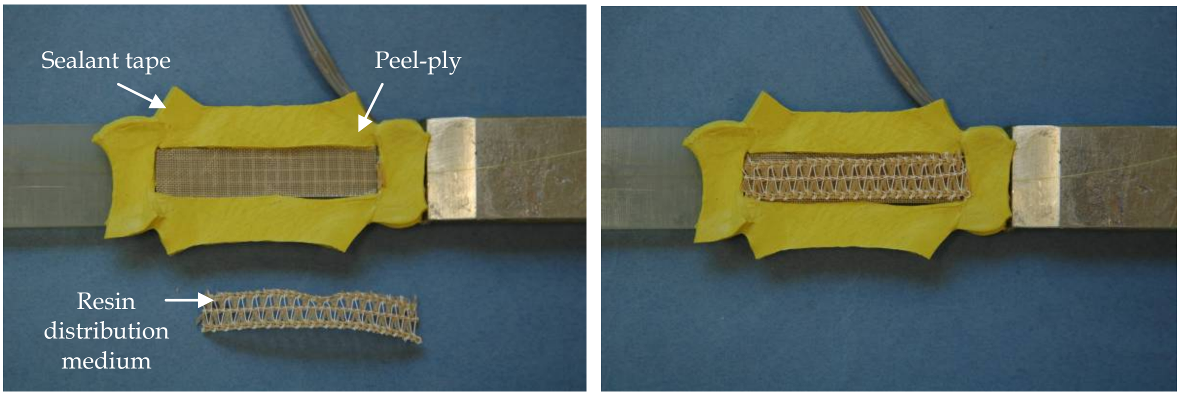

Figure 5.3: Stage two of the VATRM bonding technique (creating a seal around the fibre, peel ply and resin distribution medium using vacuum sealant tape).

Resin intake and outlet ports are constructed from the tips of two plastic syringes. The tips are cut off and trimmed to a diameter of 15 mm (Figures 5.4(a) to (c)). The edges on either side of the tip are then cut to create a gap for the fibre to pass under as shown in Figure 5.4 (c). Sealant tape is then placed around the edges of each cap leaving a short section exposed (Figure 5.4(d)) in order to allow resin to pass through. The two ports are placed at either end of the lay-up as shown in Figure 5.5.

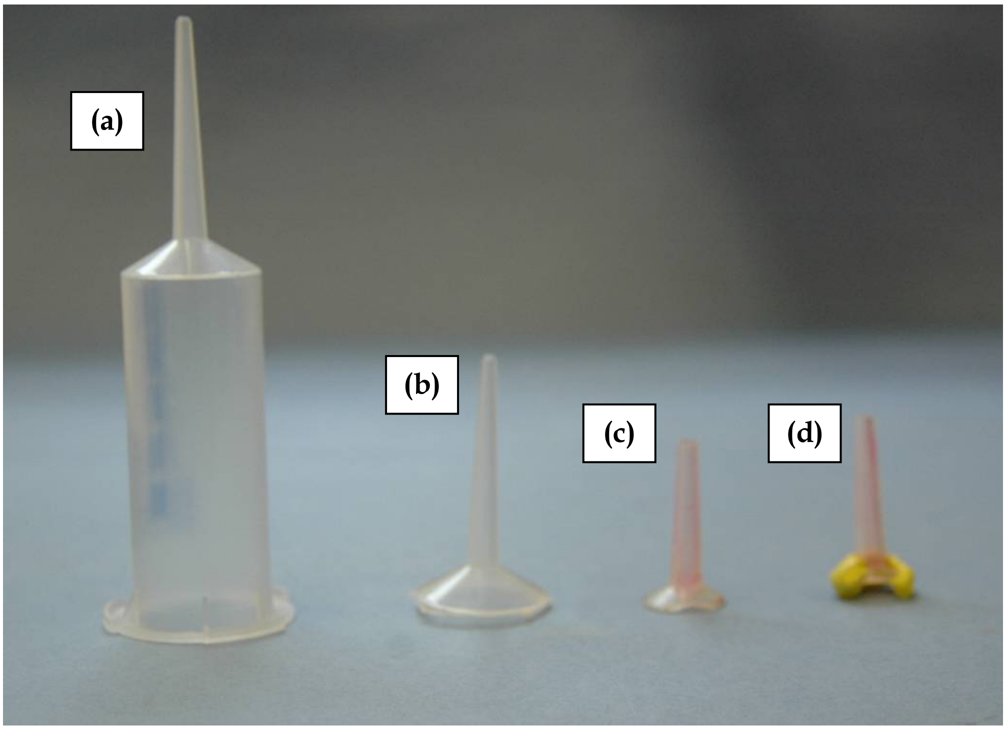

Figure 5.4: (a) Syringe; (b) Cap cut from the syringe; (c) Cap trimmed to a diameter of 15 mm with cut edges; (d) Cap with vacuum sealant tape ready to be placed on coupon.

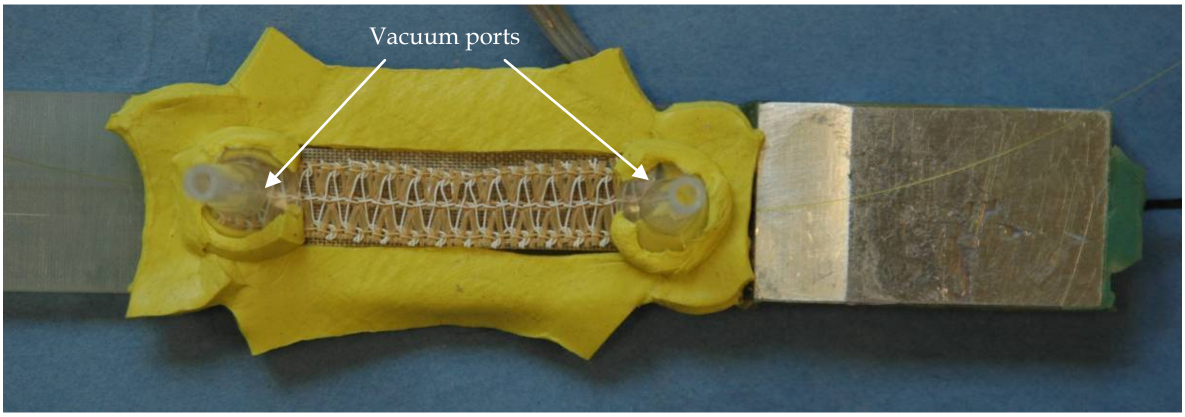

Figure 5.5: Stage three of the VARTM bonding Technique (ports placed at either end of the lay-up to allow resin to flow through).

The lay-up is sealed by a piece of vacuum bagging film with holes cut to fit over the ports as shown in Figure 5.6. A spatula is used to apply pressure to the vacuum sealant tape, especially around the edges to reduce the chance of air gaps.

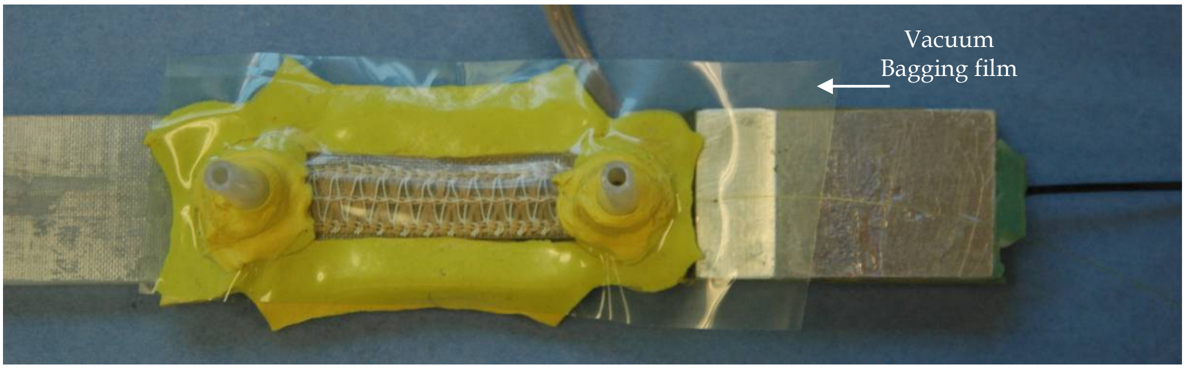

Figure 5.6: Stage four of the VARTM bonding Technique (sealing the lay-up).

The same epoxy resin was used for the small-scale VARTM infusions as was used for the large scale demonstration (Fibre Glass International Resin: R180 and Hardener: H180 slow in a 5:1 ratio of R180 to H180). To minimise the risk of air in the resin BYK550 air release was added to the resin and the mix was degassed in a vacuum chamber prior to resin infusion. A small amount of red dye was also added to the resin to improve the visibility of any air bubbles which may be present in the resin and to track the course of the resin flow. To perform the resin infusion, a vacuum line is connected to one of the ports while the other port is connected to a resin reservoir as shown in Figure 5.7. A vacuum is gradually applied at around -5 kPa and the resin flow observed to check for air bubbles which are usually an indicator of a vacuum leak in the sealant tape. These can be removed by applying further pressure to the tape to seal the gaps or reducing the vacuum. The resin flows through the lay-up and is left to dry for over an hour. Once the resin has solidified, the coupon is disconnected from the vacuum and placed in an oven to post-cure at 40 °C for at least 24 hours. Finally the sacrificial layers are removed leaving only the optical fibre and the Gyprock tape embedded in resin as shown in Figure 5.8. When using un-jacketed fibre, care must be taken when peeling off the tape, especially near the ends so as not to damage or break the fibre.

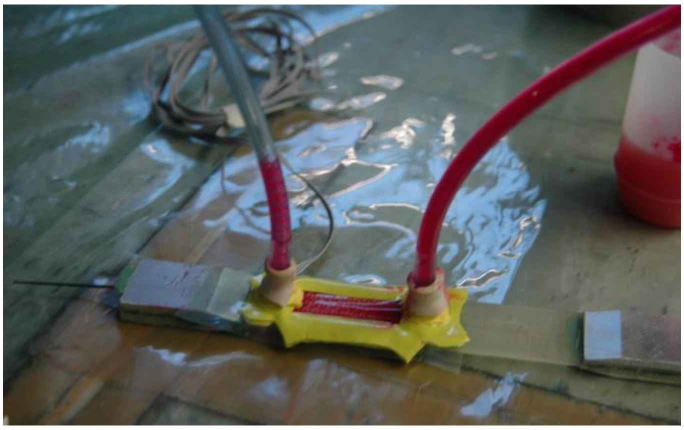

Figure 5.7: Stage six of the VARTM bonding Technique (The FBG covered with resin between the two ports).

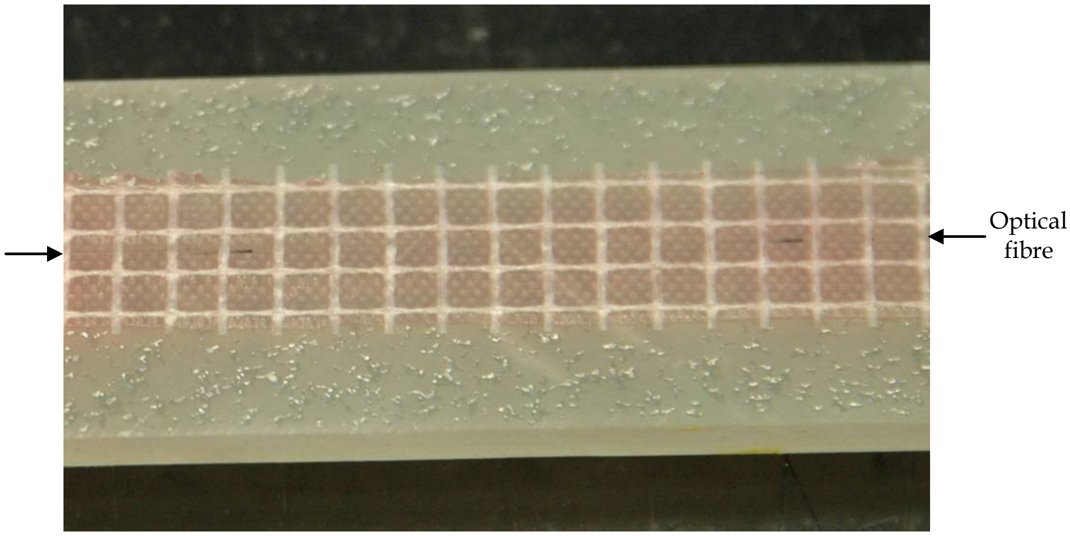

Figure 5.8: Final Product of the VARTM (optical fibre adhered to a fibre glass text coupon).

5.2.2 Redux Tape

For the fabrication of small scale Redux tape packages for the optical fibres, the same core plate was used as for the longer tape lengths, however only a short section of each channel was used as shown in Figure 5.9 (a). Using the same process as previously described in Section 2 the optical fibres are firstly laid up under tension on the Teflon lined core plate. A dam is built using vacuum sealant tape around the fibre area which is to be packaged and then one or more plies of the nylon woven tape impregnated with Redux cut to the required length are laid on top of the fibre as shown in Figures 5.9 (a)-(d). The film is cured at 120 °C under vacuum resulting in a thin flexible tape section with a very thin (10 µm approx.) resin layer between the fibre and the bottom-side of the tape. This tape can then be secondarily bonded to the coupon using standard strain gauge adhesive (MBond-200 or AE10) as shown in Figure 5.10.

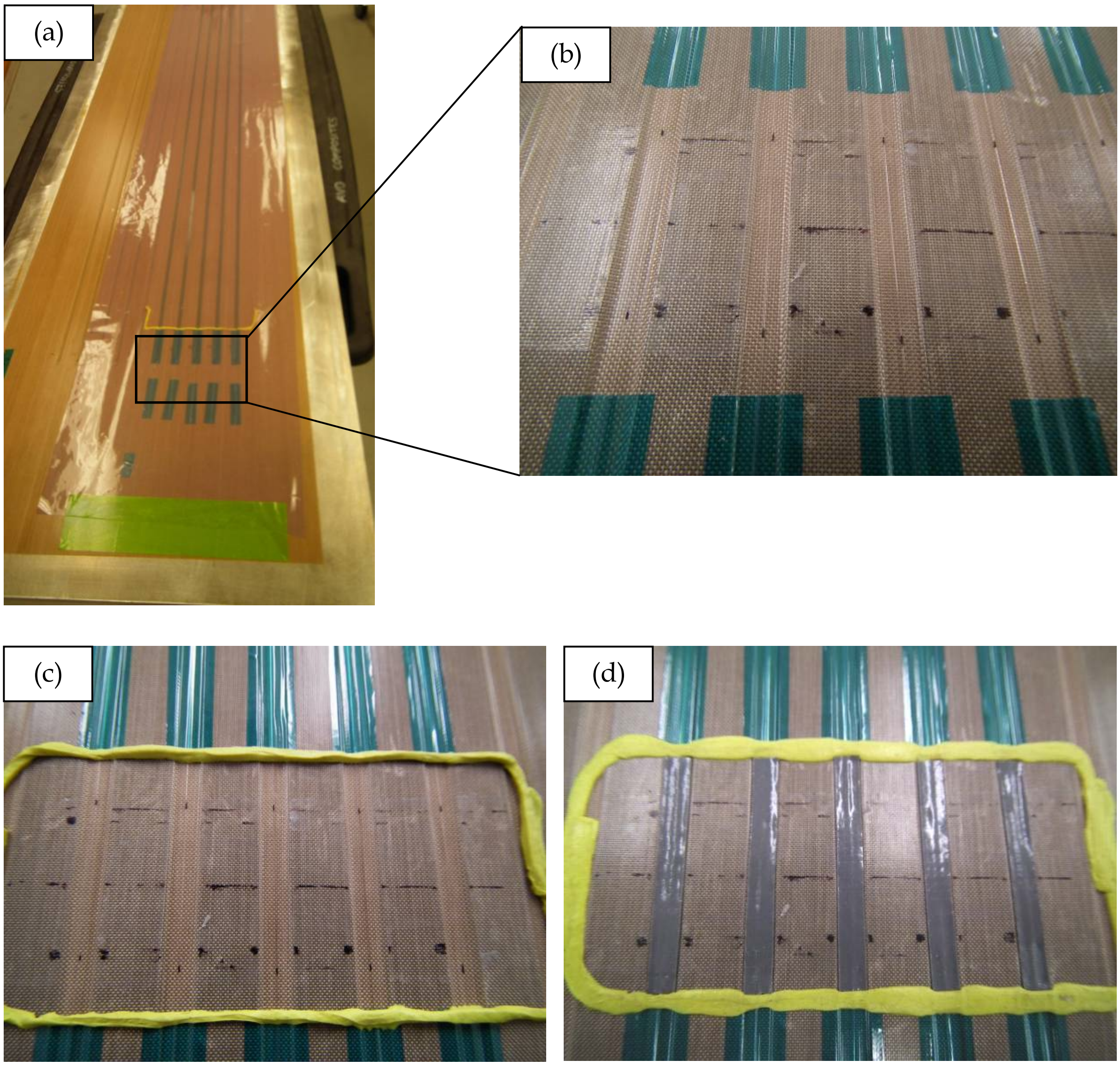

Figure 5.9: (a) Small section of core plate masked for short tape sections; (b) Optical fibres laid along the base of each channel; (c) Sealant tape placed around tape sections; (d) One or more layers of Redux tape place on top of optical fibre in channel.

(a)

(b)

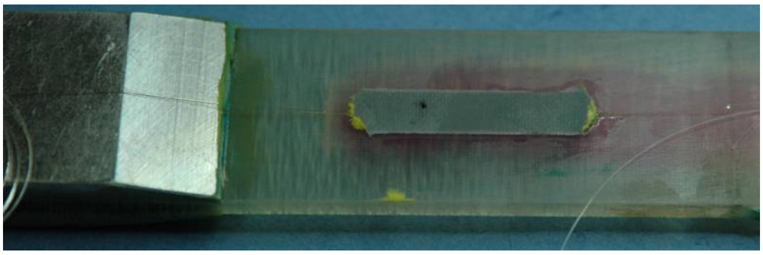

Figure 5.10: (a) FBG packaged in cured Redux tape, sealant tape residue acts as strain relief at fibre egress point); (b) Redux tape secondarily bonded to GFRP test coupon.

5.2.3 Embedded FBGs

In addition to the surface mounted gratings, some of the GFRP test coupons contained an unpackaged grating embedded between plies 6 and 7 of the composite lay-up. The FBGs in the PI coated fibre, which had their coating removed via acid or thermal stripping, were embedded in the centre of the coupon (100 mm and 12.5 mm from short and long edge respectively) running parallel to the long edge of the coupon.

5.3 Stage 1 Testing

The initial testing stage was designed to investigate the effect of different coating removal techniques on the tensile strength of optical fibres. It involved determining the strain to failure of a series of optical fibres with a section of the coating removed using the various processes outlined in Section 4.1, prior to inscription of the FBG using a standard phasemask exposure technique. In total, 30 FBGs were tested using the five different coating removal techniques. The FBGs were either surface mounted or embedded between plies 6 and 7 of the unidirectional GFRP test coupons. Both the VARTM and Redux packaging techniques were used to surface mount the FBGs to the coupons. An electrical resistance foil gauge was also surface mounted to each coupon to provide a second independent measurement of strain.

5.4 Stage 2 Testing

The second stage testing used the data from the first stage testing to determine which of the fibre stripping methodologies resulted in the most durable gratings and compared the performance of these FBGs to gratings written during the fibre draw process (DTGs). The testing was conducted in two parts; extended range strain-to-failure testing on a series of 28 cross-ply coupons and sinusoidal fatigue loading in tension to a peak strain 10,000 με on a series of 26 uni-directional coupons. A single FBG or DTG was surface-mounted front and back to each coupon using the previously described VARTM and Redux packaging techniques as shown in Figure 5.11.

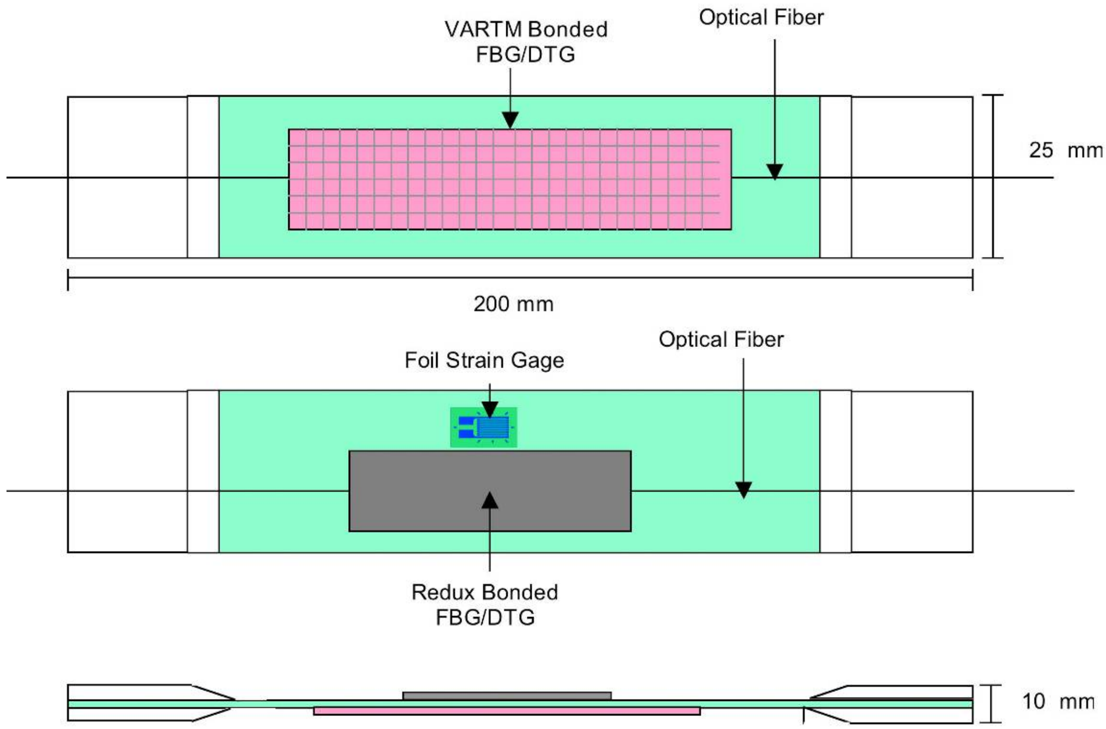

Figure 5.11: Top, bottom and side views of GFRP coupon showing placement of packaged and bonded sensors.

The VARTM packaging was bonded directly to the test coupon using the resin infusion process. The Redux tapes were cured with the optical fibre embedded and then secondary bonded to the coupon using a strain gage certified adhesive (M-Bond 200).

5.5 Experimental Methodology

Each test coupon was loaded in tension using either a 50 kN or 100 kN mechanical testing machine (depending on the load limit for the test) as shown in Figure 5.12.

In order to facilitate a semi-automated test regime, each optical fibre bonded to the test coupon was connected to an optical fibre switchbox. For the Stage 1 tests a static strain survey was conducted while the reflection spectrum from each fibre was automatically measured at 1 kN load intervals until fibre failure using a broadband Amplified Spontaneous Emission (ASE) source and an optical spectrum analyser. The foil strain gauge was connected to a digital strain indicator and manually recorded separately also at 1 kN intervals.

The strain to failure tests for Stage 2 of the testing were conducted in a similar manner except that there were no foil gauges applied due to the high strain levels. The fatigue testing for the Stage 2 tests subjected test coupons with DTGs to cyclic sinusoidal tensile loading at 6 Hz until all fibres failed or 1 million cycles was reached. The coupons were cycled in tension to a peak strain of 10,000 με. The 6 Hz cyclic rate was chosen as the highest rate that would not induce significant heating in the coupon. This was determined by cycling a coupon at a range of frequencies while measuring the surface temperature of the coupon with a thermocouple. The cap of 1 million cycles was chosen as a compromise to maximise the number of coupons which could be tested within the duration of the program. The testing was completed in blocks with periods of cyclic loading separated by static strain surveys (loading in 5 kN intervals up to 10,000 με) with the DTGs interrogated using an optical spectrum analyser to check for deterioration of the reflection spectrum. During cyclic loading periods, the dynamic strain response of the DTGs was measured using a commercial Bragg Grating interrogation system (Smart Fibres, Wx-Series). This allowed the number of cycles until failure to be determined by identifying the time at which the sensor response dropped out (i.e. the fibre failed).

Figure 5.12: Test coupon with surface mounted FBGs in a 50 kN MTS system.

6. Results

6.1 Stage 1

Figure 6.1 shows the average strain-to-failure of the FBGs written into pre-fabricated telecommunications grade optical fibre using a variety of different coating removal techniques. The error bars on the results denote the standard deviation of the data and indicate that there is a large degree of variation in strain-to-failure for each coating removal method. In addition the overall strain to failure is significantly lower than the predicted strain to failure for a pristine optical fibre which has less than 0.1% probability of failure at 500 kpsi (50,000 με) for standard telecoms fibres [8]. Overall the CO_2 Laser ablated fibres demonstrated the highest strain-to-failure of all the coating removal techniques investigated and this coating removal method was used for comparison in the second stage tests.

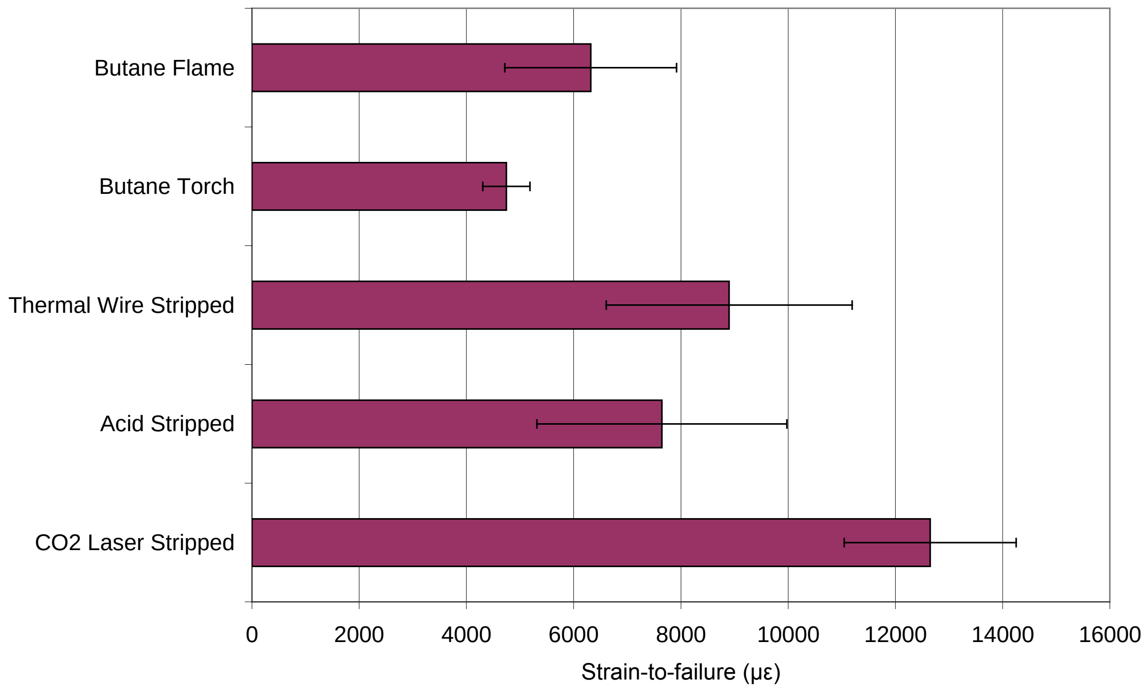

Figure 6.1: Average strain-to-failure for different coating removal techniques. Error bars indicate standard deviation of results for each measurement group.

6.2 Stage 2

Figure 6.2 shows the average strain-to-failure levels for the FBGs written in CO_2 laser stripped optical fibre and the DTGs in both the VARTM and Redux packaging. The results indicate that for both packaging techniques, the strain-to-failure for the DTGs is approaching the expected level for that of the pristine optical fibre. Importantly, the strain-to-failure levels for the FBGs in laser stripped fibre are significantly lower than for the DTGs, with the average strain-to-failure of stripped FBGs reaching only 30% of the DTG average.

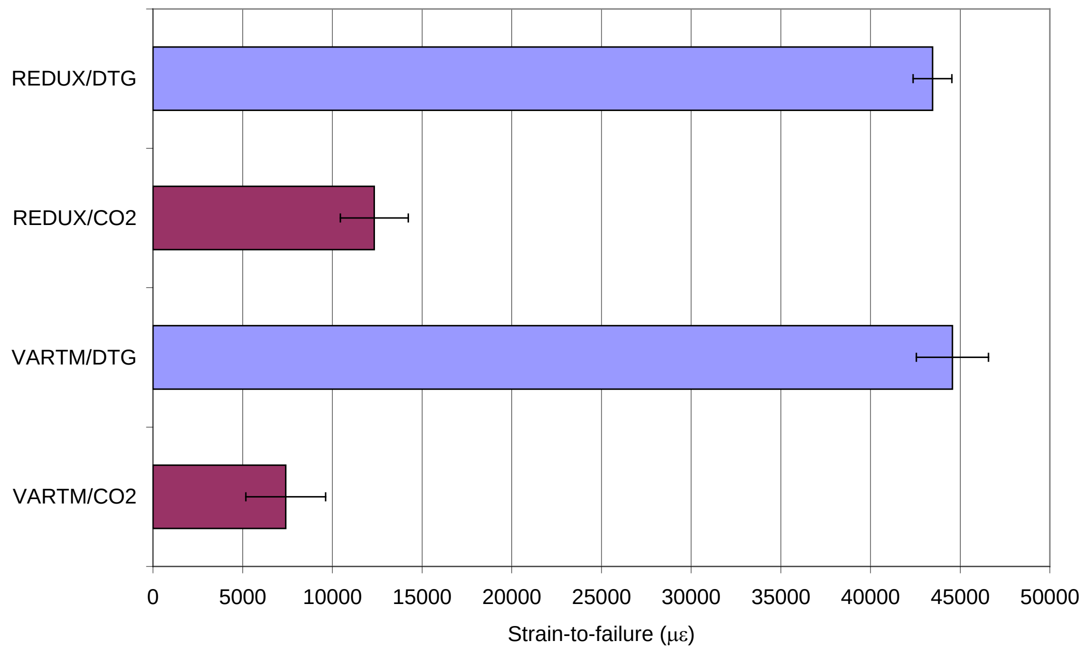

Figure 6.2: Comparison of average strain-to-failure for DTGs and CO_2 laser stripped FBGs in Redux and VARTM packaging (14 FBGs tested for each group).

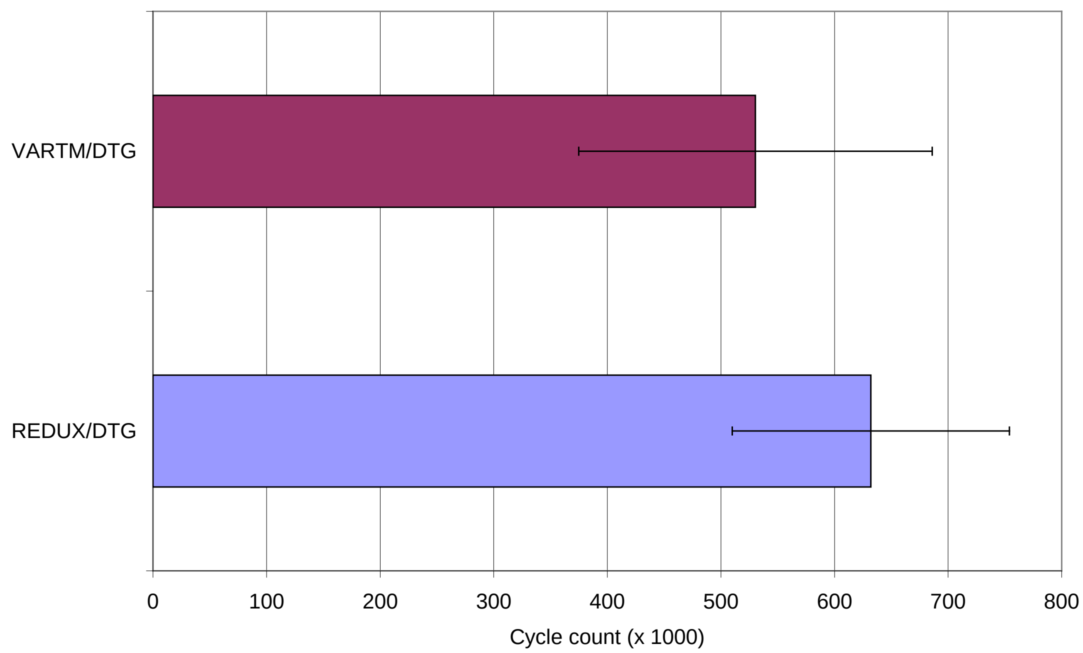

Figure 6.3: Comparison of average fatigue life for DTGs in Redux and VARTM packaging (Redux: 21 FBGs tested, VARTM: 12 FBGs tested).

Figure 6.3 shows the fatigue life (no. of cycles) for DTGs subjected to tensile fatigue loading to 10,000 με, where the fatigue life is defined as the point of optical fibre fracture. The average fatigue life for the VARTM packaged DTGs is 520,000 cycles whereas it is 620,000 cycles for the Redux packaged fibres. The results indicate that the Redux packaging performs slightly better than the VARTM packaging under these fatigue loading conditions. As the fatigue loading progressed there was also evidence of strain gradients along the length of the grating as indicated by peak splitting of the FBG reflection spectra, particularly for the VARTM packaging.

7. Analysis

7.1 Strain-to-failure tests

Figure 7.1 shows a histogram of the strain-to-failure results for DTGs. The relative standard deviation of VARTM packaged DTGs was 9% and for Redux DTGs was 5%. Both data sets exhibit an approximately normal distribution with a relatively small standard deviation, which indicates that DTG sensors fail in a consistent manner with both types of packaging.

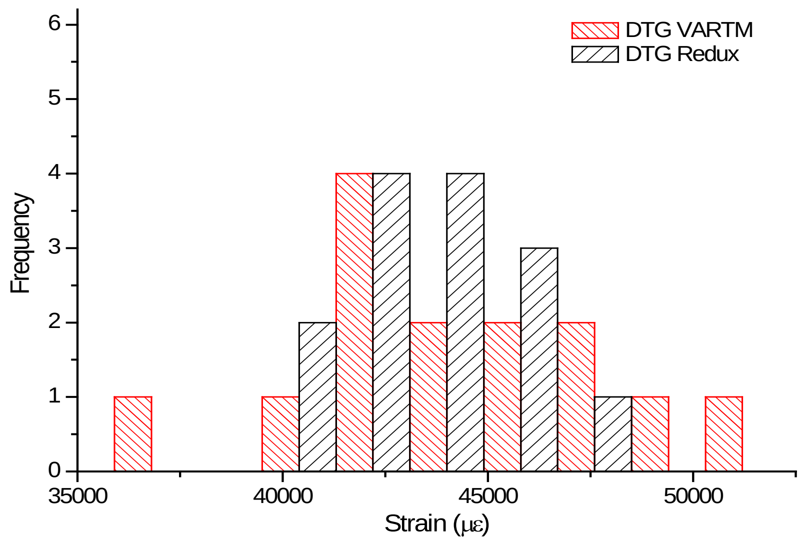

Figure 7.1: Histogram of average strain-to-failure for DTGs in Redux and VARTM packaging.

Figure 7.2 shows a histogram of the strain-to-failure results for the FBGs in CO_2 laser stripped fibre. The Redux packaged laser stripped gratings had a relative standard deviation of 31% and for the VARTM laser stripped gratings it was 60%. Both data sets have widely spread asymmetric distributions, demonstrating that the stripped and re-coated gratings do not fail in a consistent manner as the DTGs did.

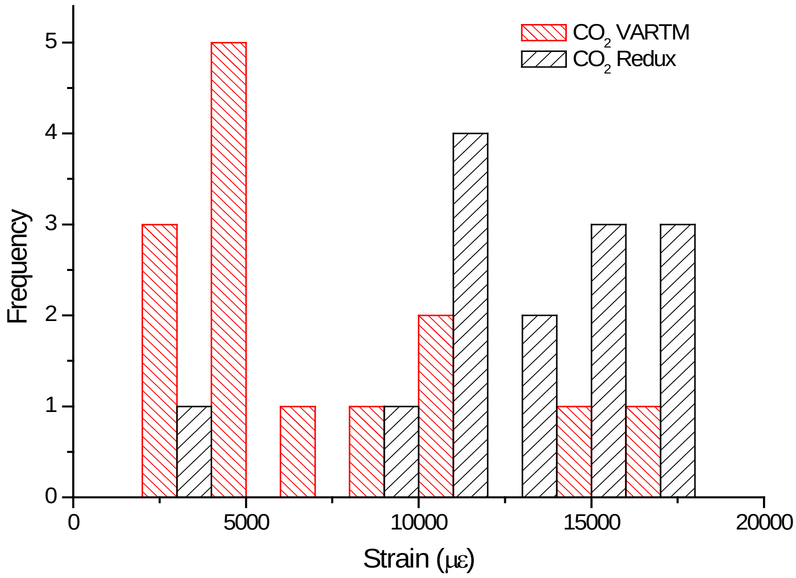

Figure 7.2: Histogram of average strain-to-failure for CO_2 laser ablated FBGs in Redux and VARTM packaging.

It is likely that the sensitivity of the stripped fibre to manual handling contributed to the less reliable results. As previously described in Section 4.1, these gratings are fabricated by ablating the protective coating surrounding the fibre using a CO_2 laser. Exposing the bare fibre leaves it susceptible to contamination from the environment and to physical damage during manual handling, especially during the packaging stage.

There is a also large difference within the results of the CO_2 stripped fibre between the VARTM and Redux packaging. VARTM packaged FBGs have a relative standard deviation approximately twice that of the Redux packaged FBGs. This is most likely due to the fact that VARTM packaging process requires a greater amount of manual handling of the fibre during its application. The exposure of the grating to the atmosphere between fabrication and packaging combined with its exposure to potential contaminants during the lay-up process appears to affect the performance of the gratings written in CO_2 stripped fibre. Such problems do not arise with VARTM when using DTGs as the entire fibre is coated.

7.2 Fatigue tests

In general, as the fatigue loading of the FBGs progressed their measured reflection spectra under load were observed to deteriorate over time prior to failure of the fibre. This deterioration presented as a gradual progression from a single peak narrow band Gaussian reflection profile as shown in Figure 7.3 (a) to a broader non-uniform spectral profile as shown in Figure 7.3 (b).

The broader non-uniform spectral profiles with reduced peak intensity are typically an indication of non-uniform strain profiles being experienced by the FBGs over the length of the gauge. It was thought that the cause of this irregular strain was most likely due to micro-cracking in the resin matrix surrounding the optical fibre.

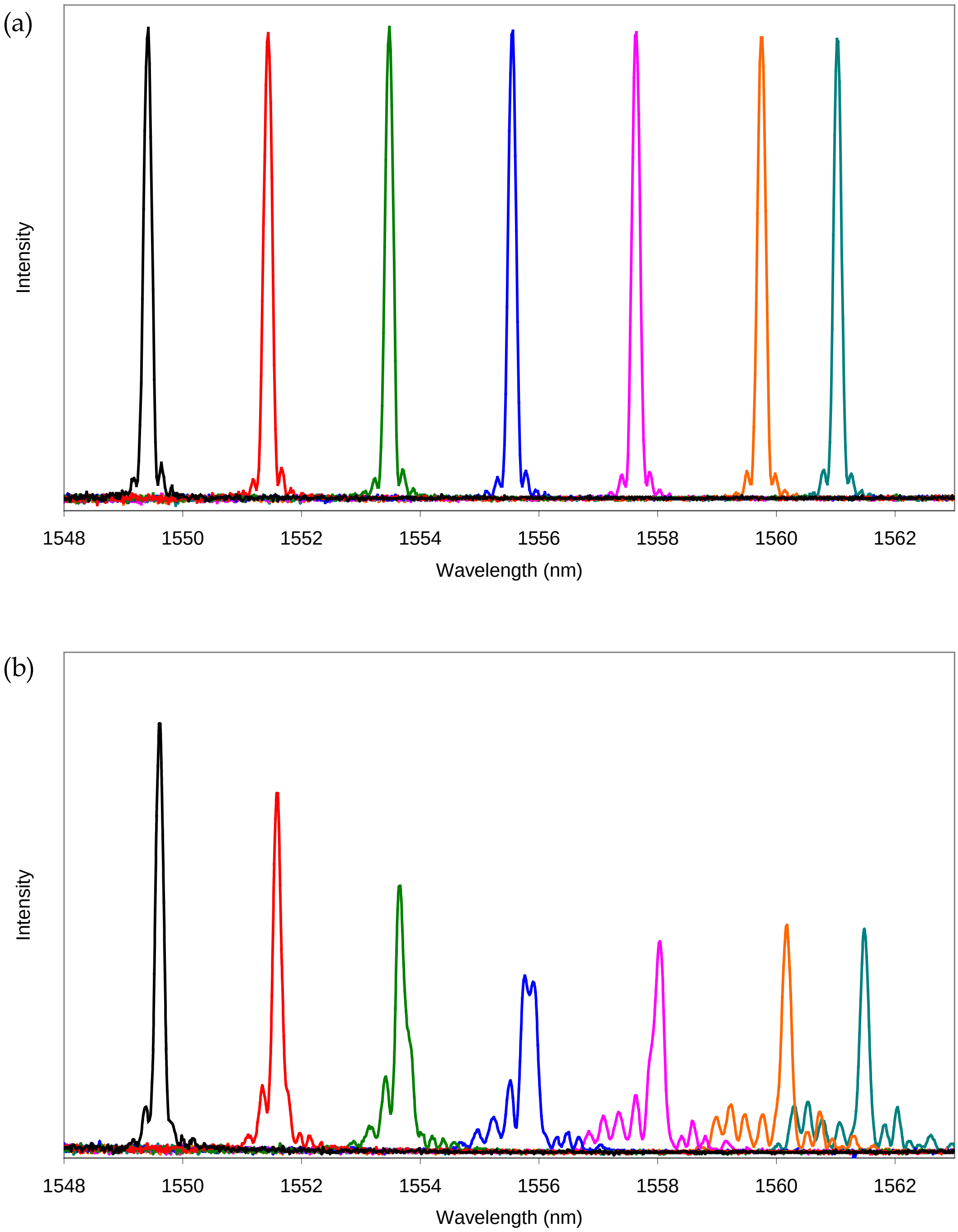

Figure 7.3: Static strain survey of surface mounted FBG up to 10,000 $\mu\varepsilon$. (a) Prior to fatigue cycling; (b) After 300 thousand cycles.

A microscopic examination of the packaging was conducted in order to verify whether this was the case. Figure 7.4 shows an enlarged image of the VARTM packaging with cracking evident running parallel to the ply weave and perpendicular to the direction of the principle load. Figure 7.3 shows cracking in the Redux packaging. A visible light source was used to locate the break in the optical fibres post-failure. This revealed that the failure point usually occurred at a micro-crack where a region of localised high strain is likely to occur. Figure 7.5 shows the visible light source relative to a micro crack. In general, the Redux packaging appeared less prone to the development of irregular strain transfer than the VARTM packaging which may be due to the fact that the resin matrix is more ductile.

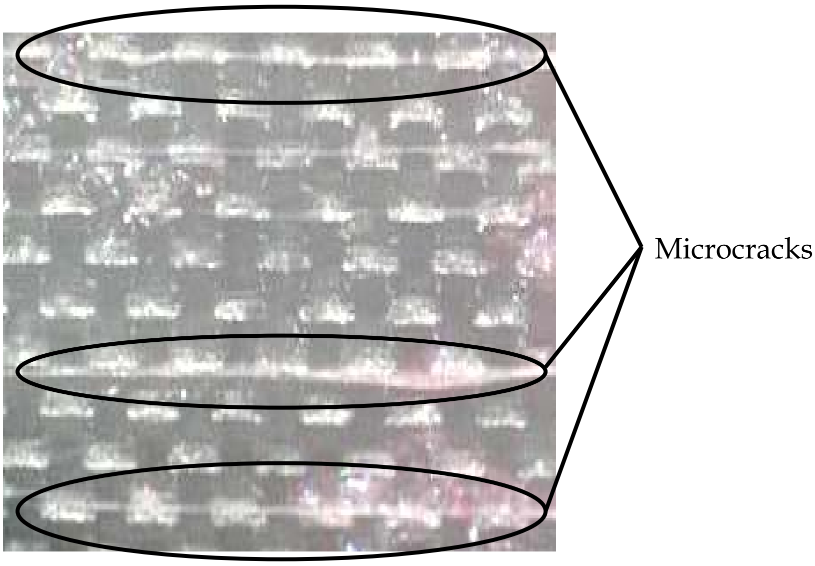

Figure 7.4: Cracking in VARTM packaging. (N.B. Imprint visible on surface is caused by the 'peel-ply' sacrificial layer).

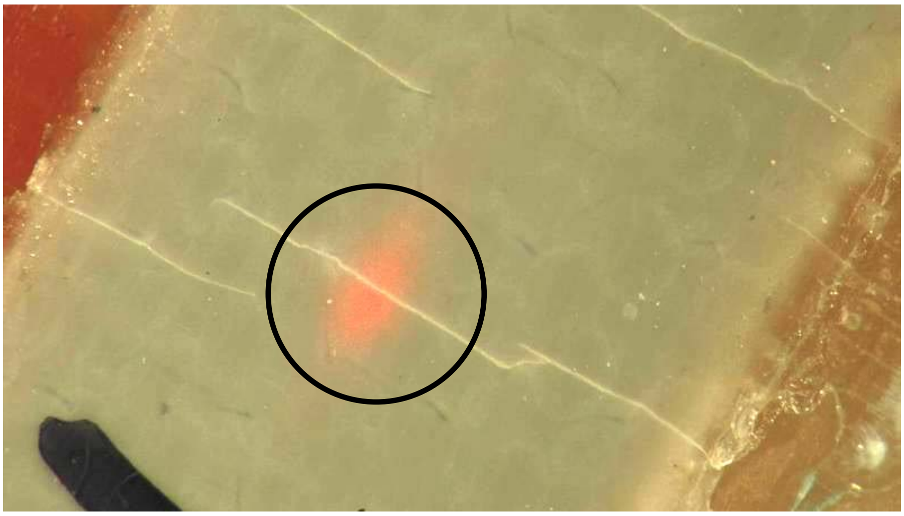

Figure 7.5: Fractures in Redux packaging. The red light seen in the highlighted region in the centre of the patch is the visible source escaping at the point of fracture in the optical fibre.

8. Conclusions

The results of this investigation into the effect of the manufacturing process on the reliability and durability of FBGs clearly show that DTGs demonstrate significantly better performance than FBGs which have been written into stripped and re-coated fibres. Five different coating removal methodologies were investigated and in all cases the average strain-to-failure was less than 30% of the average strain-to-failure for the DTGs. Overall the CO_2 laser ablated fibres demonstrated the highest strain-to-failure of all the stripped and re-coated FBGs.

Two broad area packaging techniques were developed for the purpose of retrofitting DTG sensing arrays to Defence Platforms, namely: VARTM and Redux. Single DTG sensors were sinusoidally fatigue loaded to 10,000 $\mu\varepsilon$ using both surface-mount packages. The average fatigue life for the VARTM packaged DTGs was 520,000 cycles whereas it is was 620,000 cycles for the Redux packaged fibres.

With recent enhancements in DTG fabrication technology, the reflectivity of these gratings should be sufficient for use with most commercially available FBG interrogators.

Additional benefits that DTGs offer over stripped and recoated gratings include:

- A more streamlined and less labour intensive manufacturing process which may lead to economies of scale.
- The ability to write long arrays of FBGs without an increased risk of breaking or damaging the entire array.
- No risk of contamination and a greatly reduced risk of damage through manual handling.

For these reasons, the use of DTGs should be considered a priority on Defence platforms for structural health monitoring applications where long-term use in harsh environments is required. At present, to the best of the author's knowledge there is only one commercial manufacturer of high reflectivity DTGs (FBGS Technologies), which presents a certain level of fragility in this area. However, there is potential for more wide spread commercialisation of the process when the patent on the fabrication process expires in a few years. It is likely that the new adopters of this technology will first emerge in China.

For situations where DTGs cannot be utilised for whatever reason, careful consideration should be given to the fabrication process employed by the manufacturer and the performance specifications supplied for the sensors. The results in this investigation show that there is a large degree of variability in the performance of stripped and re-coated gratings which is influenced by the both the coating removal technique and the handling and storage process during fabrication. This is probably a contributing factor to the large range of results which have been reported in the literature in the area of FBG reliability [9–13].

The preferred packaging process largely depends on the targeted platform, the intended position of the sensors, the sensor count and the conditions under which the sensors are expected to operate. Although both types of packaging developed under this research program showed evidence of cracking under fatigue loading, the strain levels applied (10,000 $\mu\varepsilon$) were well in excess of what would typically be experienced on most military platforms currently in service. In general, VARTM is more suited to rigid structures and broad area applications, as long strands of sensor arrays can be rolled out onto a structure and then infused without any additional heating. Redux is more suited to small clusters of sensors, less accessible locations or less rigid structures, as Redux patches have greater ductility and a small footprint.

9. Future Work

Although the preliminary results for the both the Redux and VARTM packaging combined with the DTGs are promising and indicate good reliability and durability at relatively high strain levels, to date, no work has been conducted looking at the performance of these packages under peel and shear loading conditions. In addition the packaging has not been exposed to adverse environmental conditions such as excessive salinity, humidity or thermal cycling. Before this packaging can be considered for long-term use on Defence platforms a study into the potential effects of these factors should be conducted.

The only method investigated in this study to secondarily bond the cured Redux tape to a structure has been using M-bond 200 adhesive. This method is adequate for short lengths of Redux tape, but not suitable for long tape lengths. Further investigation into co-curing Redux tape directly to structures or techniques for secondary bonding long tape lengths with a uniform bond line would prove advantageous for in-field application of Redux tape.

10. Acknowledgements

The authors gratefully acknowledge the Office of Naval Research for the support of this work under the Naval International Cooperative Opportunities in Science and Technology Program (Grant No. N00014-09-1-0364; program sponsor Dr. Ignacio Perez). The authors would also like to acknowledge Mr. Chris Hamill for assistance with the composites fabrication and Swinburne University for providing access to the CO_2 laser stripper.

11. References

[1] G. Meltz, W.W. Morey, W.H. Glenn, and J.D. Farina. In-Fibre Bragg-grating temperature and strain sensors. *Proceedings of the ISA Aerospace Instrumentation Symposium*, Vol. 34, pp. 239-242, 1988.

[2] J.R. Sayre. Vacuum-Assisted Resin Transfer Molding (VARTM) Model Development, Verification, and Process Analysis. Virginia Polytechnic Institute and State University, Ph.D. thesis, 2000.

[3] I. Grabovac, T. Nuyens and C. Davis. Packaging and Mounting of In-Fibre Bragg Grating Arrays for Structural Health Monitoring of Large Structures. DSTO-TR-2490. Defence Science and Technology Organisation, 2010.

[4] Redux® 322 Modified epoxy film adhesive. Hexcel Corporation. 2008. http://www.hexcel.com/Resources/DataSheets/Adhesives-Data-Sheets/322_eu.pdf

[5] C. Chojetzki, M. Rothhardt, J. Ommer, S. Unger, K. Schuster and H.R. Mueller. High-reflectivity draw-tower fibre Bragg gratings - arrays and single gratings of type II. *Optical Engineering,* Vol. 44, No. 6, 060503-060503-2, 2005.

[6] N. Mrad, S. Sparling, and J. Laliberte. Strain monitoring and fatigue life of Bragg grating Fibre optic sensors. *Proceedings of SPIE - The International Society for Optical Engineering*, Vol. 3670, pp. 82-91, 1999.

[7] P.R. Stoddart, C. Davis, S. Wade, and A. Mazzolini. FigFab: Fibre Bragg Grating Fabrication and Collaborative Research at Swinburne University. *Proceedings of the 1st Pacific International Conference on Applications of Lasers and Optics*, Melbourne, Australia, 2004.

[8] R.J. Castiglione, G.S. Glaesenam, and T.A. Hanson. Extrinsic Strength Measurements and Associated Mechanical Reliability Modelling of Optical Fibre. *National Fiber Optics Engineers Conference,* Vol. 16, pp. 1-9, 2000.

[9] Y.J. Rao. In-fibre Bragg grating sensors. *Measurement science and technology,* Vol. 8, No.4, pp. 355, 1997.

[10] H.J. Yoon, and C.G. Kim. The mechanical strength of fiber Bragg gratings under controlled UV laser conditions. *Smart materials and structures,* Vol. 16, No. 4, pp. 1315-1319, 2007.

[11] D.H. Kang, S.O. Park, C.S. Hong, and C.G. Kim. Mechanical strength characteristics of fiber Bragg gratings considering fabrication process and reflectivity. *Journal of Intelligent Material Systems and Structures,* Vol. 18, No. 4, pp. 303-309, 2007.

[12] A.J. Tarpey, S.N. Kukureka, and K. Jurkschat. The mechanical reliability of stripped and recoated polyimide fibers for optical fiber sensors. *Proceedings of SPIE (Optical Fiber and Fiber Component Mechanical Reliability and Testing II),* Vol. 4639, pp. 141-151, 2002.

[13] J. Ang, H.C.H Li, and I. Herszberg. Tensile fatigue properties of fiber Bragg grating optical fiber sensors. *International Journal of Fatigue*, Vol. 32, No. 4, pp. 762-768, 2010.

DEFENCE SCIENCE AND TECHNOLOGY ORGANISATION
DOCUMENT CONTROL DATA

1. PRIVACY MARKING/CAVEAT (OF DOCUMENT)

2. TITLE

Reliability, Durability and Packaging of Fibre Bragg Gratings for Large-Scale Structural Health Monitoring of Defence Platforms

3. SECURITY CLASSIFICATION (FOR UNCLASSIFIED REPORTS THAT ARE LIMITED RELEASE USE (L) NEXT TO DOCUMENT CLASSIFICATION)

Document	(U)
Title	(U)
Abstract	(U)

4. AUTHOR(S)

Claire Davis, Ivan Grabovac, James Kopczyk,
Peter Lombardo, Patrick Norman, Anthony Rizk,
Travis Nuyens and Silvia Tejedor

5. CORPORATE AUTHOR

DSTO Defence Science and Technology Organisation
506 Lorimer St
Fishermans Bend Victoria 3207 Australia

6a. DSTO NUMBER	6b. AR NUMBER	6c. TYPE OF REPORT	7. DOCUMENT DATE
DSTO-TR-2880	AR-015-684	Technical Report	August 2013

8. FILE NUMBER	9. TASK NUMBER	10. TASK SPONSOR	11. NO. OF PAGES	12. NO. OF REFERENCES
2013/1087863/1	ERP 07/250	ONR	35	13

13. DSTO Publications Repository

http://dspace.dsto.defence.gov.au/dspace/

14. RELEASE AUTHORITY

Chief, Aerospace Division

15. SECONDARY RELEASE STATEMENT OF THIS DOCUMENT

Approved for public release

OVERSEAS ENQUIRIES OUTSIDE STATED LIMITATIONS SHOULD BE REFERRED THROUGH DOCUMENT EXCHANGE, PO BOX 1500, EDINBURGH, SA 5111

16. DELIBERATE ANNOUNCEMENT

No Limitations

17. CITATION IN OTHER DOCUMENTS Yes

18. DSTO RESEARCH LIBRARY THESAURUS http://web-vic.dsto.defence.gov.au/workareas/library/resources/dsto_thesaurus.shtml

Bragg Gratings, Structural health monitoring, Reliability

19. ABSTRACT

This report documents an experimental program of work which investigates the reliability and durability of fibre Bragg gratings under tensile loading conditions and the factors which contribute to their ultimate performance. In addition, methodologies for broad-area permanent attachment of FBG sensing arrays are also investigated and two techniques are presented for proposed application in the structural health monitoring of Defence platforms.